Electronic supplementary information

Bioinspired chemoenzymatically controlled artificial light harvesting nanoaggregates with multicolour transient emissions for time-gated information encryption

Priyam Das, Sampurna Routray, Ritvika Kushwaha, Malay Kumar Baroi, Debapratim Das*

Experimental

General

Benzophenone, 4-hydroxybenzophenone, 4,7-dithien-2-yl-2,1,3-benzothiadiazole (DBT), Rhodamine B (RhB) and Nile red (NR) were purchased from TCI Chemicals (India) were purchased from Tokyo Chemical Industry (TCI) Chemicals (India). Ethyl 4-bromobutyrate was purchased from Sigma-Aldrich (USA). Urease ex. Jack Beans (Activity: 394 U/mg) and urea were purchased from SRL. Tris(hydroxymethyl)aminomethane (TRIS), NaOH, tri-Sodium citrate dihydrate and Citric acid monohydrate were purchased from Merck. Titanium tetrachloride was purchased from Spectrochem. Milli-Q water with a conductivity of<2μScm^{-1} was used for all sample preparations and experimental measurements. 60-120 mesh silica gel (SRL) was used for column chromatography. ^{1}H NMR and ^{13}C NMR spectra were recorded using a Bruker Ascend 600 MHz (Bruker, Coventry, UK) spectrometer. Coupling constants (J values) are reported in hertz, and chemical shifts are reported in parts per million (ppm). FESEM imaging was performed on a Gemini SEM 300 (Sigma Zeiss) instrument. The particle size analyses were performed at 298 K using Zetasizer Nano-ZS90 (Malvern). A He–Ne LASER (λ=632.8 nm) was used as an excitation source for dynamic light scattering (DLS) measurements. UV–vis spectra (absorbance and transmittance) were recorded on a PerkinElmer Lambda 365+ spectrometer. Fluorescence measurements were performed on a Fluoromax 4 Plus spectrophotometer. pH data were recorded on a Hanna HI 2210 pH meter equipped with a HI1131 pH probe from Hanna. The PL decay measurements were performed using a time-correlated single photon counting (TCSPC) setup with MCP detection (Horiba Jobin, Model: Ultrafast-01-DD). An LED of 340 nm was used for the excitation of the sample. The absolute quantum yield measurements were performed using an Edinburgh Life Spec II instrument. The chromaticity diagram and CIE coordinate points were plotted with SpectraChroma.

Synthesis

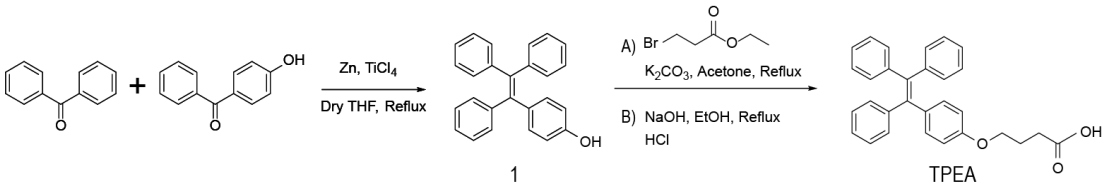

Scheme S1. Synthetic Scheme for the preparation of TPEA

Synthesis of Compound 1

Zinc powder (1.65 g, 25 mmol, 10 equiv.) was measured in a double-necked 100 mL round-bottom flask equipped with a magnetic stirrer and purged with Argon. Dry THF (20 mL) was added to it. The mixture was stirred at 0 °C in an ice bath for 30 minutes. $TiCL_4$ (1.4 mL, 12.5 mmol, 5 equiv.) was added slowly to it with a syringe in the argon medium at 0 °C. The suspension was gradually allowed to reach room temperature, after which it was refluxed for 3 hours. The suspension was again cooled to 0 °C in an ice bath and stirred. A solution of benzophenone (250 mg, 1.37 mmol, 1 equiv.) and 4-hydroxybezophenone (270 mg, 1.37 mmol, 1 equiv.) in THF (10 mL) was added dropwise to this suspension under cold conditions and stirred in the ice bath for 30 minutes after complete addition. The reaction mixture was then refluxed for 6 hours. The reaction mixture was cooled and concentrated, and then diluted with EtOAc. The EtOAc fraction was washed thrice with saturated $NaHCO_3$ solution and concentrated to obtain the crude product. The crude product was purified over a column with 10% EtOAc in Hexane to obtain the pure product as a white powder (Yield ~ 51 %). ^{1}H NMR (600 MHz, Chloroform-*d*): δ 7.12 – 7.06 (m, 9H), 7.05 – 6.99 (m, 6H), 6.89 (d, *J*= 8.6 Hz, 2H), 6.56 (d, *J*= 8.6 Hz, 2H), 4.80 (s, 1H); ^{13}C NMR (150 MHz, Chloroform-*d*) δ 154.41, 144.35, 144.25, 144.23, 140.79, 140.53, 136.69, 133.08, 131.71, 131.69, 131.67, 128.05, 127.95, 126.72, 126.60, 114.93; MS (ESI): m/z calculated for $C_{26}H_{20}O$: 348.15; found for $[C_{26}H_{20}O]$: 348.19.

Synthesis of Compound TPEA

Compound 1 (350 mg, 1 mol, 1 equiv.), K_2CO_3 (165 mg, 1.2 mol, 1.2 equiv.) and ethyl 4-bromobutyrate (186 μL, 1.3 mol, 1.3 equiv.) were measured in a 100 mL double-necked round-bottom flask equipped with a magnetic stirrer and purged with argon and sealed. To it, 20 mL of dry acetone was added, and the reaction mixture was refluxed for 12 hours. The reaction mixture was cooled to room temperature and concentrated, and then diluted with EtOAc. The EtOAc fraction was washed with dil. HCl and the water. The organic fraction was concentrated to obtain the crude product, which was purified over a column with 5% EtOAc in hexane to give a white powder as the pure product. The product was taken in a round-bottom flask and refluxed with NaOH (2.0 equiv.) in EtOH (15 mL) for 18 hours. The reaction mixture was concentrated under vacuum and diluted with a minimum amount of water. The solution was acidified dropwise with 6M HCl to a very low pH – 1.0. until a white turbid solution appeared. The precipitate was isolated and dried under vacuum to obtain the pure product as a white powder (Yield ~ 58 %). ^{1}H NMR (600 MHz, Chloroform-*d*) δ 7.13 – 7.06 (m, 9H), 7.05 – 6.99 (m, 6H), 6.92 (d, *J* = 8.7 Hz, 2H), 6.61 (d, *J* = 8.7 Hz, 2H), 3.94 (t, *J* = 6.0 Hz, 2H), 2.55 (t, *J* = 7.3 Hz, 2H), 2.07 (p, *J* = 6.7 Hz, 2H); ^{13}C NMR (150 MHz, Chloroform-*d*) δ 177.97, 157.61, 144.36, 144.31, 140.83, 140.46, 136.62, 132.89, 131.73, 131.70, 131.67, 128.07, 127.94, 126.70, 126.60, 126.57, 113.90, 66.65, 30.65, 24.75; MS (ESI): m/z calculated for $C_{30}H_{26}O_3$: 434.19; found for [$C_{30}H_{26}O_3$]: 434.20.

Preparation of Stock Solutions of Dyes

The stock solutions of all the fluorophore dyes were prepared in ethanol and stored at 4 °C.

Execution of Citrate-Urea/Urease pH clock

In a glass vial, 2.8 mL of water was taken, and the required volume of urease solution was added from its stock (1000 U/mL). The solution was basified to pH 9.0 with 5 μL of 1 mM NaOH solution. This was immediately followed by the simultaneous addition of required volumes of sodium citrate/citric acid buffer (pH 3.5, 100 mM stock) and urea (2 M stock) solutions. The solution was quickly homogenised with a micropipette, and then the pH change was monitored from an initial pH of 3.7 to a final pH of 8.6 over time.

Absorption measurements

All absorption experiments were recorded in a 3 mL quartz cuvette (path length 1 cm) with a slit width of 1 nm at 298 K. To 3 mL of water or buffer of desired pH, the required volume of dye was added from their respective stock solutions to obtain the desired concentrations. It was then evenly mixed with a micropipette and equilibrated for a minute before data acquisition. For a typical time-dependent experiment, all the required contents were added to a dye solution following the sequence as in the pH clock. The contents were uniformly homogenised, and the spectra were recorded at regular time intervals or at a particular wavelength over a time span as needed.

Fluorescence Measurements

All fluorescence experiments were performed in a 3 mL quartz cuvette (path length 1 cm) with a slit width of (Ex./Em.) = 2/2 nm at 298 K under λ_{ex} = 350 nm unless otherwise mentioned. For any time-independent measurements, required volumes of dyes were added to the solution in the cuvette from their respective stock solutions, mixed thoroughly, equilibrated for 1 minute and then recorded. In a typical time-dependent fluorescence experiment, all the contents were added following the same proportion and sequence as that in the pH clock. The contents were quickly homogenized with a micropipette, and then the emission spectra were recorded at intervals of every minute over 30 minutes. The final concentration of TPEA was 25 μM and was variable for variable dyes.

Time-Resolved Photoluminescence and Quantum Yield Measurements

All measurements were performed in a 3 mL quartz cuvette with a 1 cm path length. For all the experiments, the required concentration of the dyes and their combinations was maintained, respectively. For studies conducted under static pH conditions, buffers were used. For time-resolved photoluminescence lifetime measurements, a 340 nm (~100 ps, 1 MHz repetition rate) diode laser was used for excitation. A deconvolution procedure was used to analyze the observed decays, which could be satisfactorily fitted by bi-exponential decay functions. A deconvolution procedure was used to analyze decays using a proper instrument response function obtained by using a light scatterer (suspension of TiO_2 particles in water). The fluorescence decays [I(t)] were analyzed in general as a sum of exponentials. The fluorescence decays [I(t)] were analyzed in general as a sum of exponentials, [1]

$$I(t) = \sum B_i exp(-\frac{t}{\tau_i}) \qquad \text{(S1)}$$

where, B_i and τ_i are the pre-exponential factor and fluorescence lifetime for the ith component, respectively. Reduced chi-square (χ^2) values and random distribution of the weighted residuals among data channels were used to judge the acceptance of the fits.

FRET Efficiency and Förster Radius

FRET efficiency, Φ_{ET}, the fraction of the absorbed energy that is transferred to the acceptor, is experimentally measured as a ratio of the fluorescence intensities of the donor in the absence and presence of the acceptor (I_D and I_{DA}).

$$\Phi_{ET} = 1 - \frac{I_{DA}}{I_D} \qquad \text{(S2)}$$

The energy-transfer efficiency (Φ_{ET}) was calculated in pH 3.0 citrate buffer, measured for TPEA (25 μM) with different concentrations of different acceptor dyes.

To estimate the Förster radius of donor-acceptor and donor-donor, the spectral overlap integral was then calculated using the following equation:

$$J = \int_0^\infty f_D(\lambda)\varepsilon_A(\lambda)\lambda^4 d\lambda \qquad \text{(S3)}$$

Where λ is the wavelength of light (nm), $\varepsilon_A(\lambda)$ is the molar absorptivity of the acceptor at that wavelength ($M^{-1}\,cm^{-1}$), and $f_D(\lambda)$ is the donor fluorescence spectrum normalized on the wavelength scale according to

$$1 = \int_0^\infty f_D(\lambda) d\lambda \qquad \text{(S4)}$$

The overlap integral was estimated to be $9.59\times10^{14}\ M^{-1}\,cm^{-1}\,nm^4$ for transfer between TPEA and DBT, $5.56\times10^{13}\ M^{-1}\,cm^{-1}\,nm^4$ for transfer between TPEA and RhB and $4.34\times10^{12}\ M^{-1}\,cm^{-1}\,nm^4$ for transfer between TPEA and NR. The Förster radius can be calculated using the following equation:

$$R(\text{Å}) = 0.211 \times (J\varphi\,\kappa^2\eta^{-4})^{1/6} \qquad \text{(S5)}$$

κ^2 as the orientation value was assumed to be 2/3, the refractive index of solvent $\eta = 1.33$ and the fluorescence quantum yield of donor (φ) is 0.67 according to the calculation result. The Förster radius was thus estimated to be 4.8 nm, 2.9 nm and 1.9 nm for transfer between TPEA and DBT, TPEA and RhB and TPEA and NR, respectively.

FESEM and FETEM Analyses

For the time-dependent FESEM experiments, 5 μL of the sample solution under pH clock were taken out at specific times and drop-cast on a silicon wafer. The samples were immediately freeze-dried to arrest the pH clock kinetics and then analyzed. For samples under static pH conditions, 5 μL of the sample solution prepared in buffer was cast on a silicon wafer, dried, and analyzed for morphologies.

DLS Analyses

The particle sizes were recorded in a 3 mL DLS cuvette. For measurements under static pH conditions, the buffer solution of the desired pH was taken, followed by the addition of required volumes of dyes from their stock solutions. The solutions were thoroughly mixed and equilibrated for 1 minute before measurements. For a typical time-dependent dynamic experiment, all the constituents were added following the same proportion and sequence as that in the pH clock. The contents were quickly homogenized with a micropipette, and then the particle sizes were monitored at regular intervals over 30 minutes.

Time-encoded encryption in chemically triggered colour codes

For the time-regulated ASCII codes, 8 small glass cuvettes (1 cm × 1cm × 1cm) were arranged linearly side by side. Each cuvette contained clear solutions having urease and TPEA (25 μM) at pH 9.0 adjusted with dilute NaOH. pH clock was initiated in the desired cells by the addition of the citrate buffer/urea trigger, which generated turbidity in them. The time-dependent changes in the turbidity were visually observed.

For the time-regulated Morse codes, solutions of TPEA (blue) and TPEA:DBT (yellow) were placed in well plates at specific positions. In basic conditions, under UV light (365 nm), no emission was visible. When the pH clock was initiated, the blue and yellow fluorescence appeared that depicted the Morse code representations, which were time-locked and vanished temporally.

For the time-regulated transitory colour code, 16 small glass cuvettes (1 cm × 1cm × 1cm) were arranged in a 4 × 4 perfect square. Each of them was filled with 1 mL of water. Adequate volumes of desired dyes were added to them from their respective stock solutions to produce the desired colours. Under basic pH, no turbidity nor any emission was seen. Initiation of the pH clock produced turbid solutions, which appeared colour under UV light of 365 nm. The colours were time-encoded and thus vanished after the end of the cycle. The codes can be read through their colours, appearing in sequence from left to right. Each colour represents a digit (0,1, 2, 3). When read from left to right in a single row, it generates a 4-bit code from a single row. This code, when converted to its 64-base code, gives a number that encrypts for an alphanumeric character. In this way, if the entire setup is decrypted at the right time along the time-scale, it reveals a hidden message that dissipates over time. Once initiated, the entire setup was monitored over time and photographed at regular time intervals to capture the necessary change and different codes.

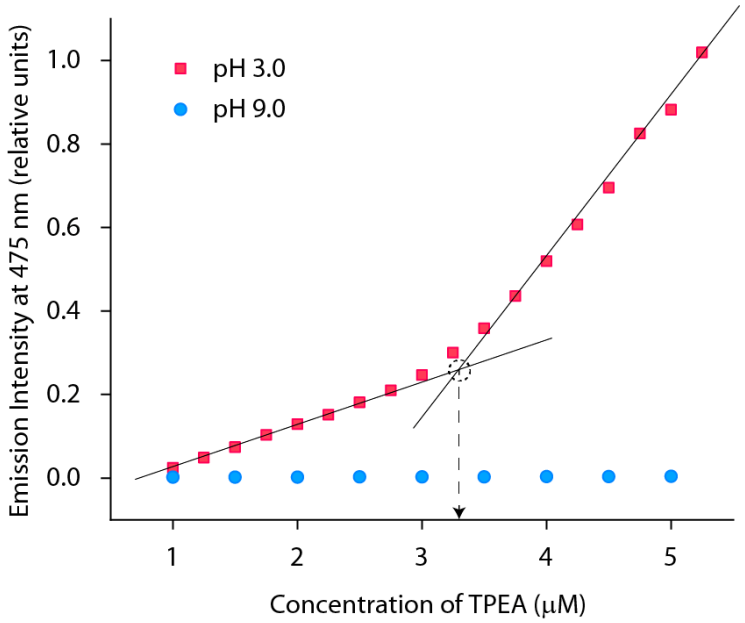

Fig. S1 pH-dependent Critical aggregation concentration of TPEA.

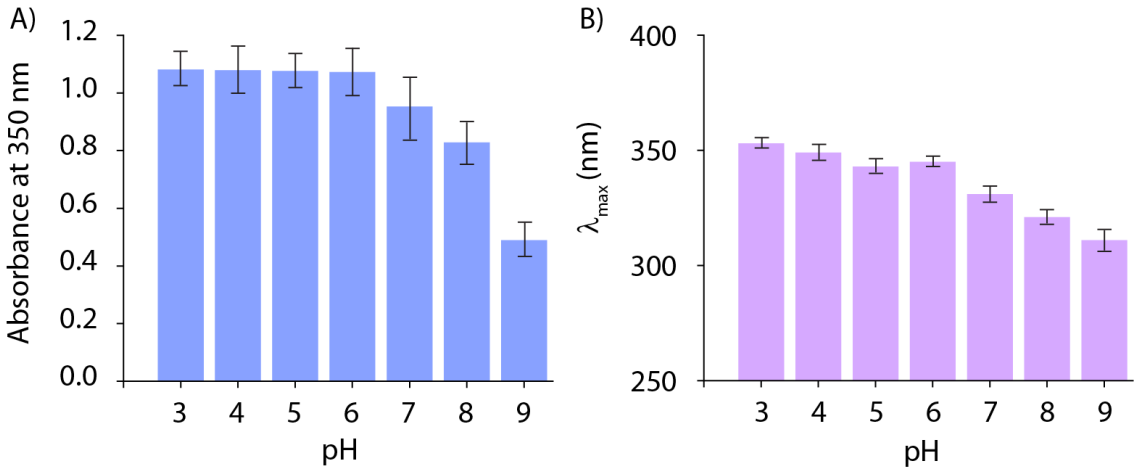

Fig. S2 pH-dependent A) absorption at 350 nm and B) wavelength of maximum absorption (λ_{max}) of TPEA (25 μM).

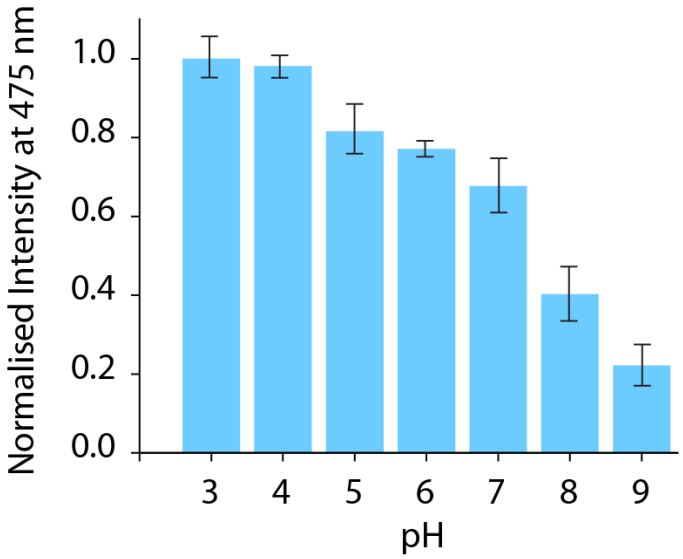

Fig. S3 Emission intensity of TPEA (25 μM) at 475 nm (λ_{em}) in solutions of different pH.

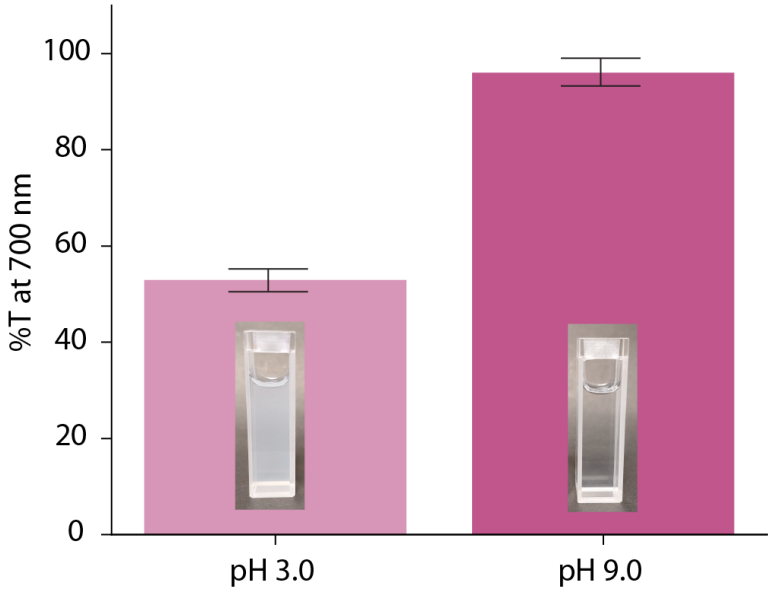

Fig. S4 Transmittance of solution of TPEA (25 μM) at 700 nm at A) pH 3.0 and B) pH 9.0.

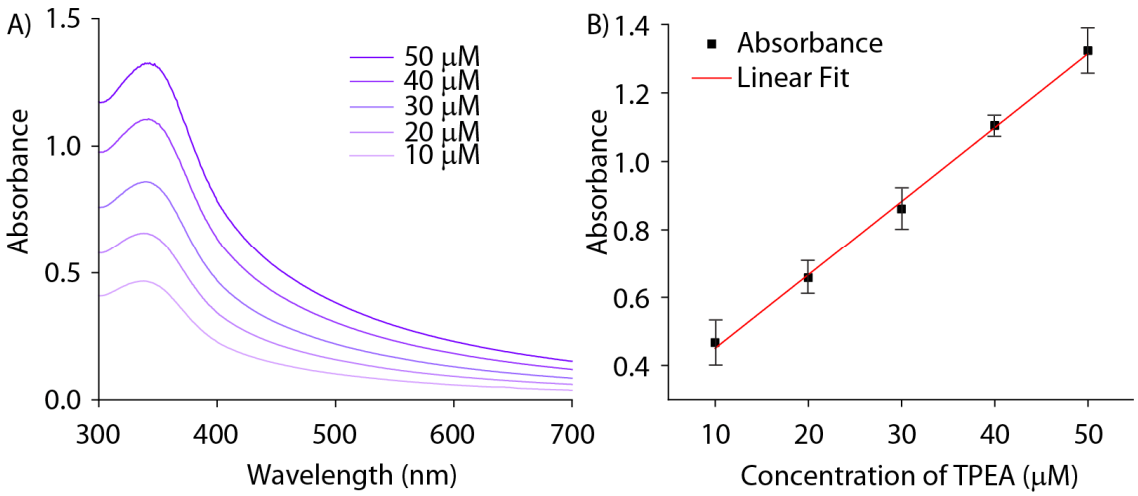

Fig. S5 A) Concentration-dependent absorption spectra of TPEA at pH 3.0. B) Linear variation of absorbance (350 nm) versus concentration of TPEA at pH 3.0.

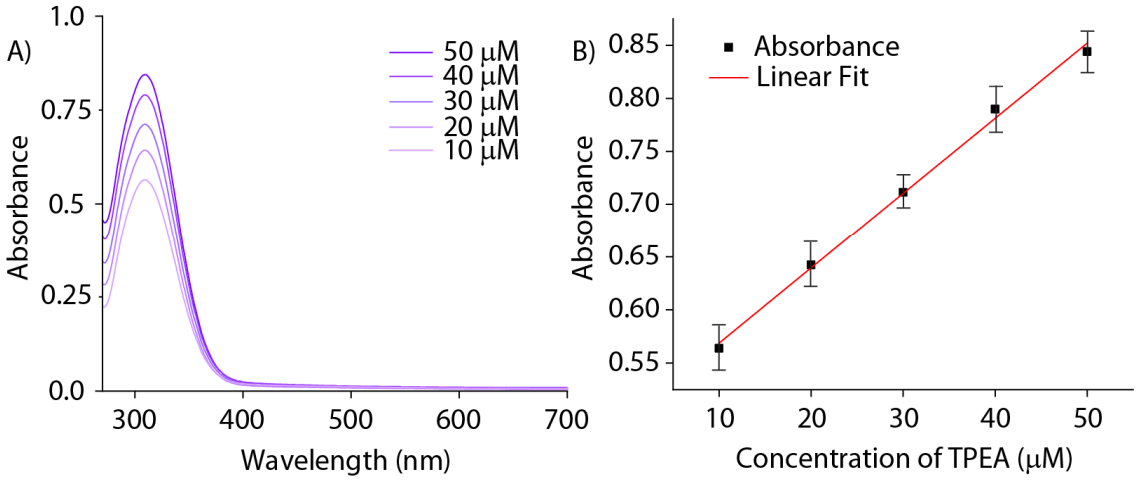

Fig. S6 A) Concentration-dependent absorption spectra of TPEA at pH 9.0. B) Linear variation of absorbance (350 nm) versus concentration of TPEA at pH 9.0.

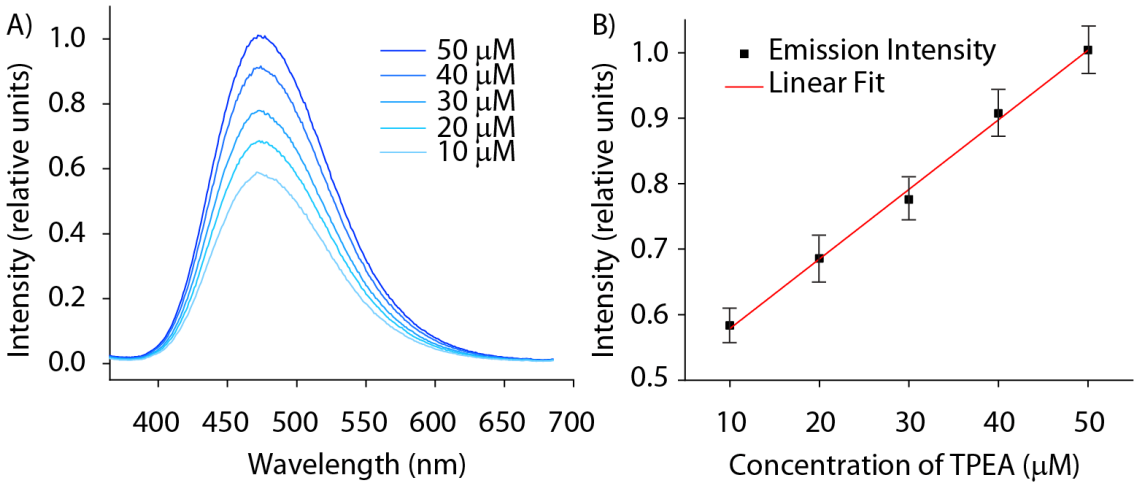

Fig. S7 A) Concentration-dependent emission spectra of TPEA at pH 3.0. B) Linear variation of emission intensity (475 nm) versus concentration of TPEA at pH 3.0.

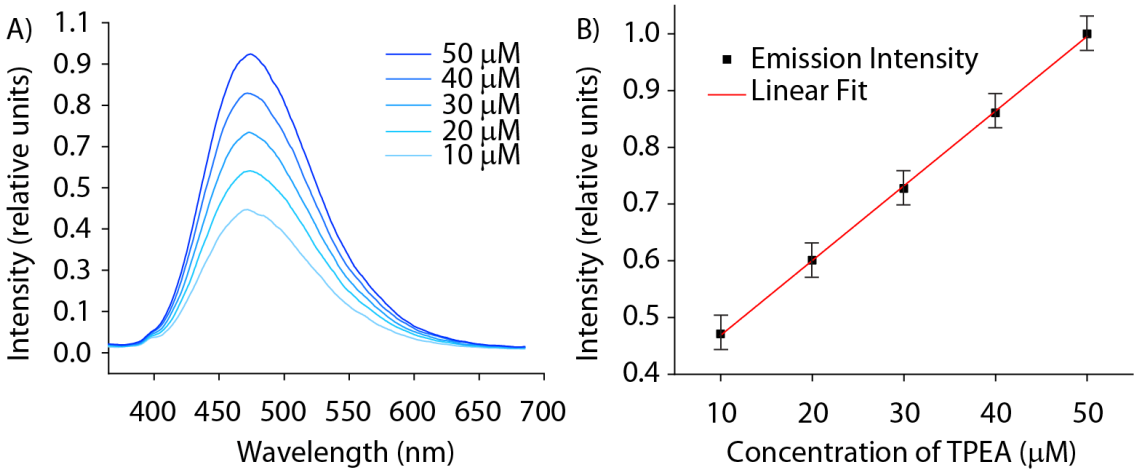

Fig. S8 A) Concentration-dependent emission spectra of TPEA at pH 9.0. B) Linear variation of emission intensity (475 nm) versus concentration of TPEA at pH 9.0.

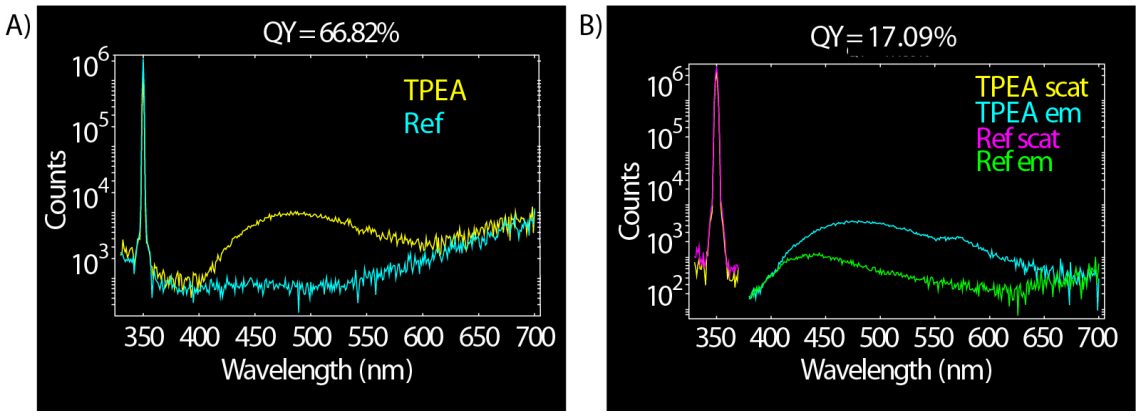

Fig. S9 Quantum yields at 475nm for TPEA (25 μM) at A) pH 3.0 and B) pH 9.0

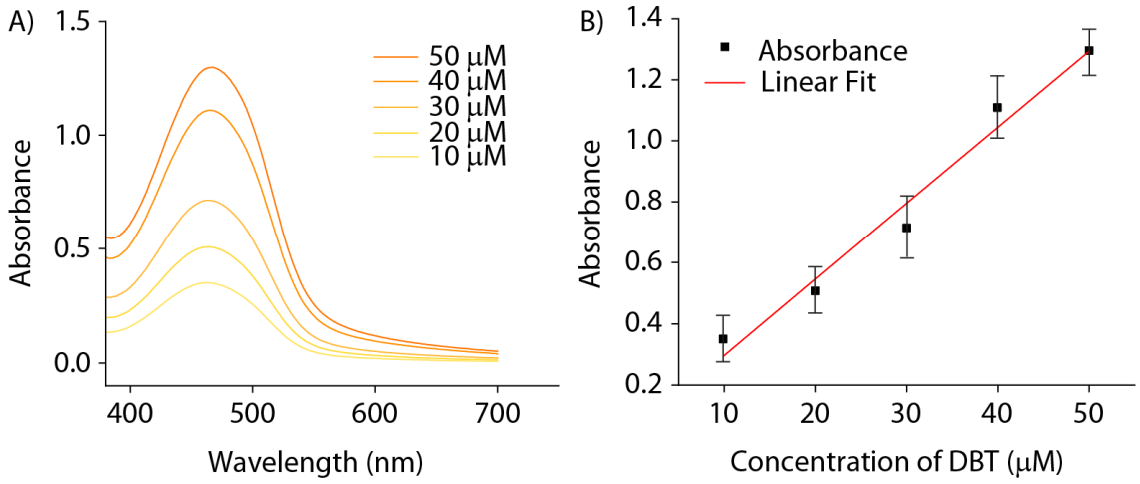

Fig. S10 A) Concentration-dependent absorption spectra of DBT at pH 3.0. B) Linear variation of absorbance (460 nm) versus concentration of DBT at pH 3.0.

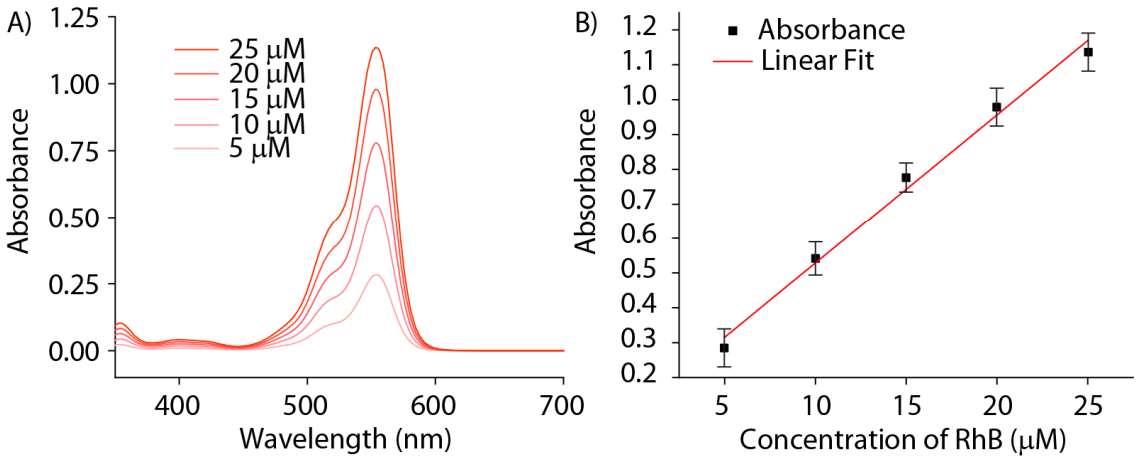

Fig. S11 A) Concentration-dependent absorption spectra of RhB at pH 3.0. B) Linear variation of absorbance (550 nm) versus concentration of RhB at pH 3.0.

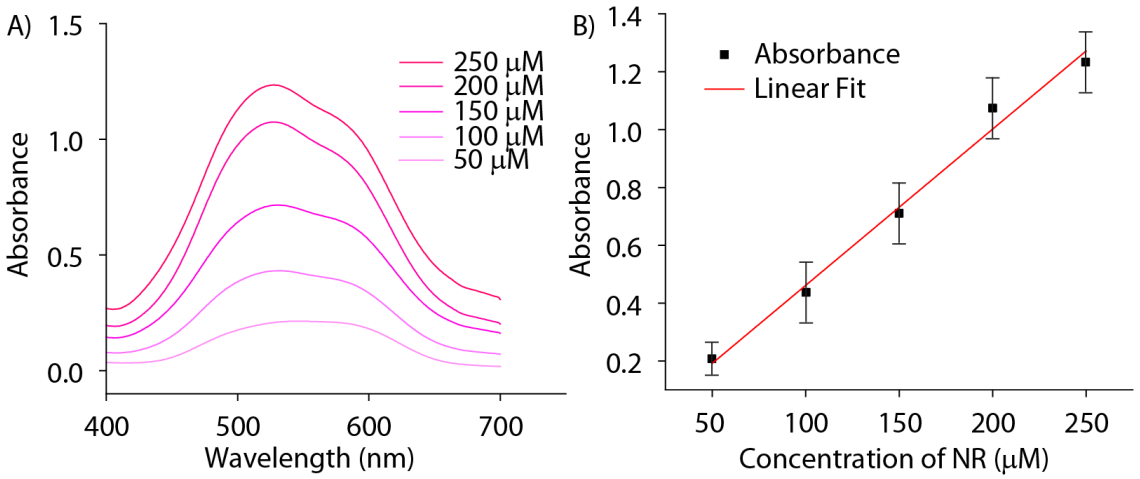

Fig. S12 A) Concentration-dependent absorption spectra of NR at pH 3.0. B) Linear variation of absorbance (525 nm) versus concentration of NR at pH 3.0.

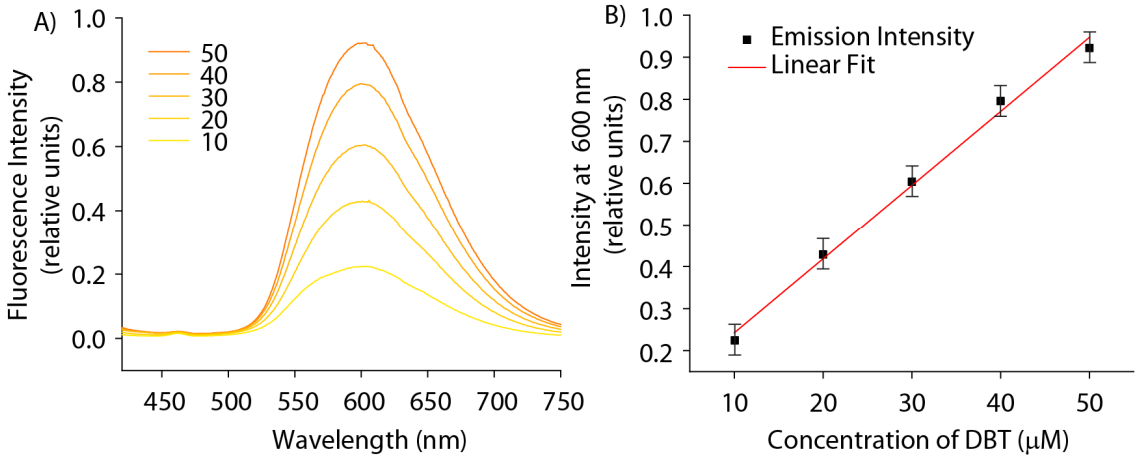

Fig. S13 A) Concentration-dependent emission spectra of DBT at pH 3.0. B) Linear variation of emission intensity (600 nm) versus concentration of DBT at pH 3.0.

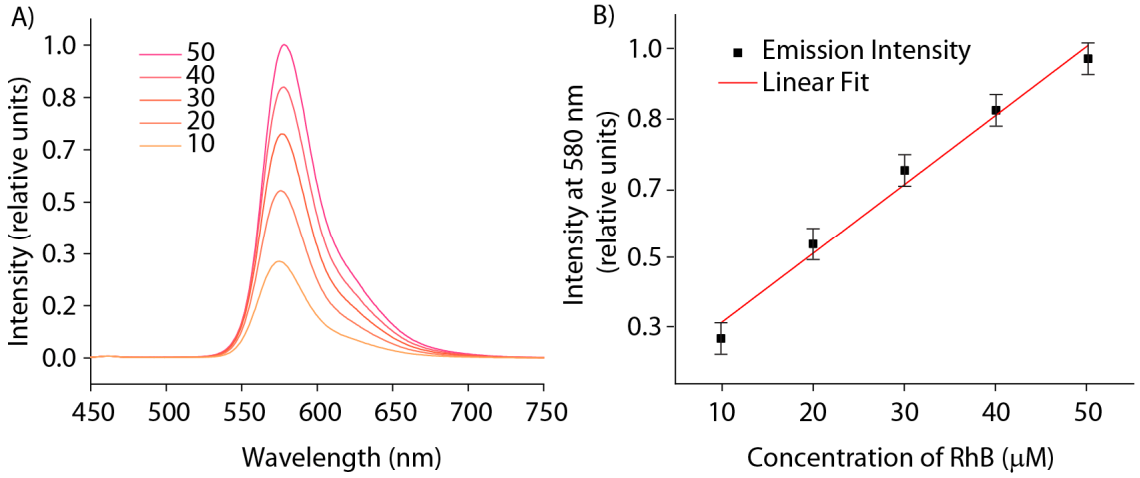

Fig. S14 A) Concentration-dependent emission spectra of RhB at pH 3.0. B) Linear variation of emission intensity (580 nm) versus concentration of RhB at pH 3.0.

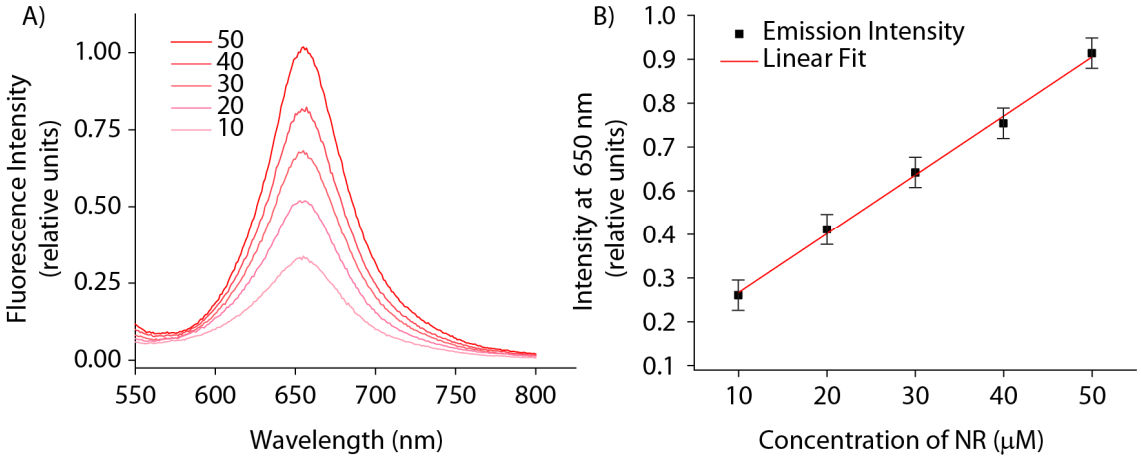

Fig. S15 A) Concentration-dependent emission spectra of NR at pH 3.0. B) Linear variation of emission intensity (650 nm) versus concentration of NR at pH 3.0.

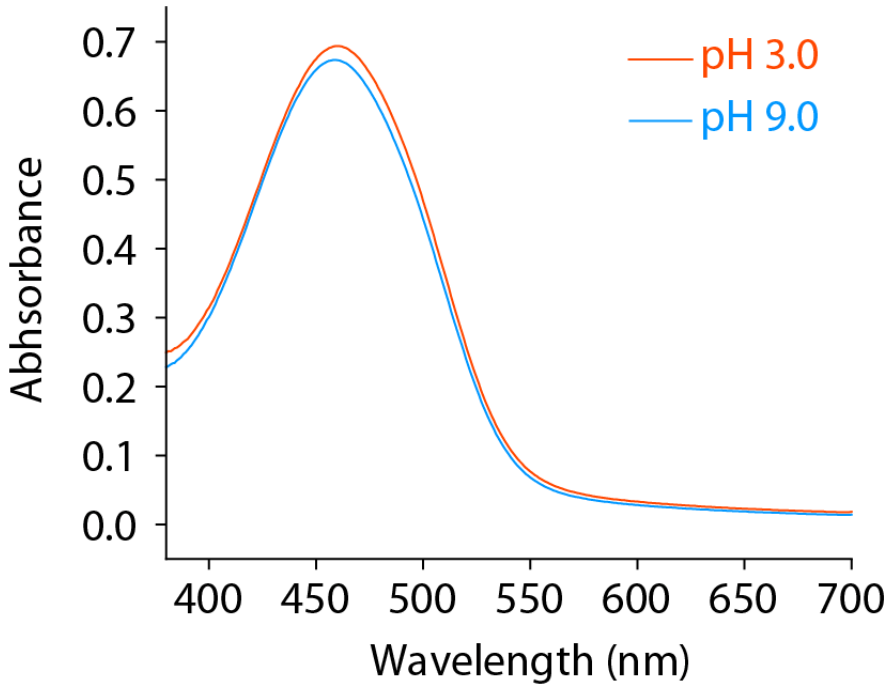

Fig. S16 pH-dependent absorption spectra of DBT (10 μM)

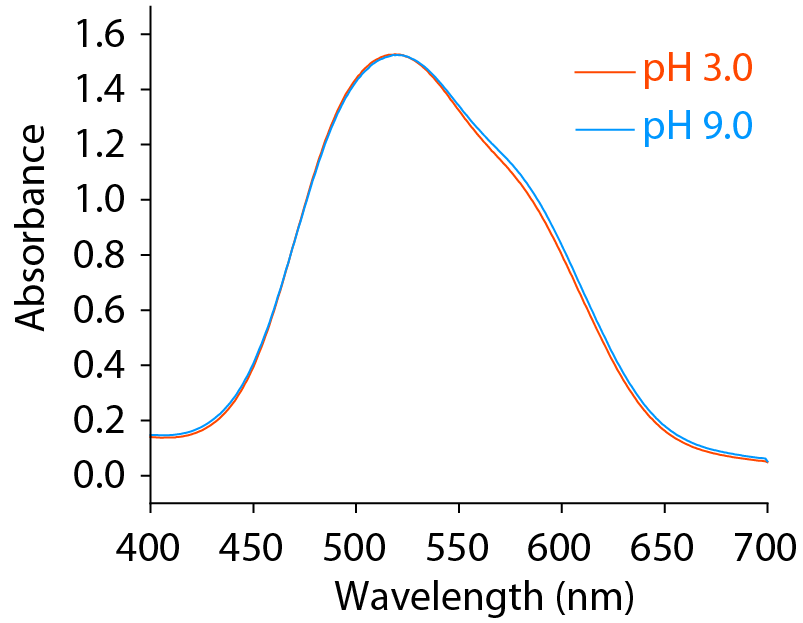

Fig. S17 pH-dependent absorption spectra of NR (10 μM)

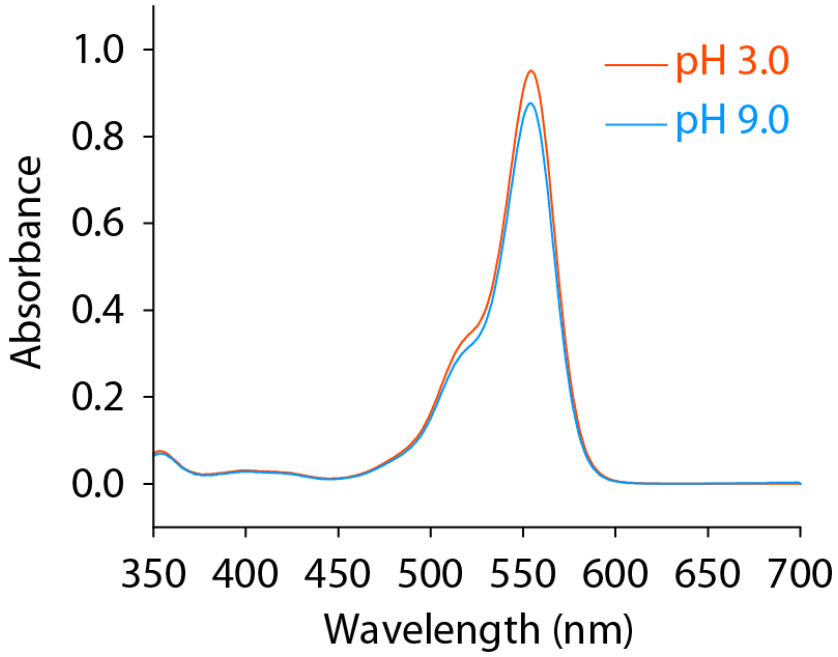

Fig. S18 pH-dependent absorption spectra of RhB (10 μM)

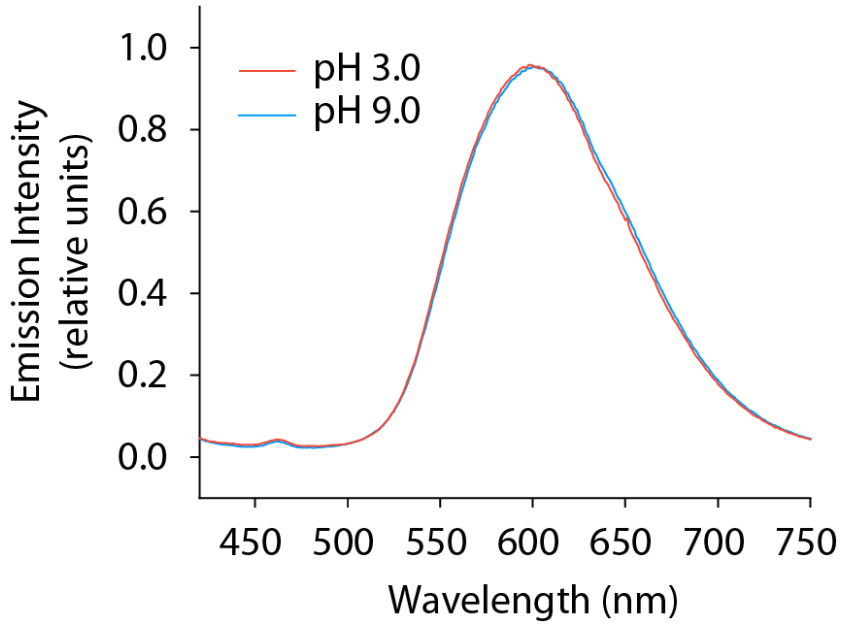

Fig. S19 pH-dependent emission spectra of DBT (10 μM).

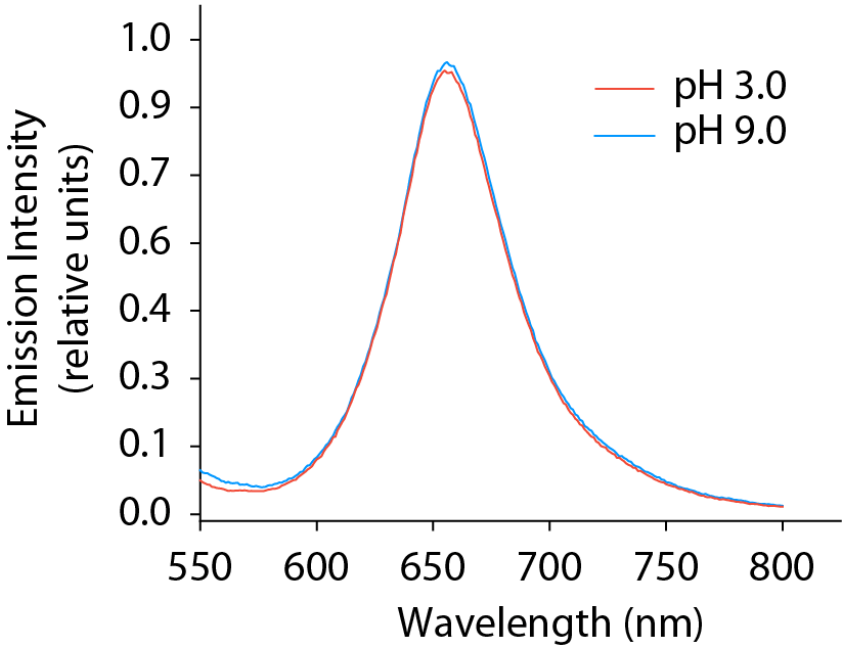

Fig. S20 pH-dependent emission spectra of NR (10 μM)

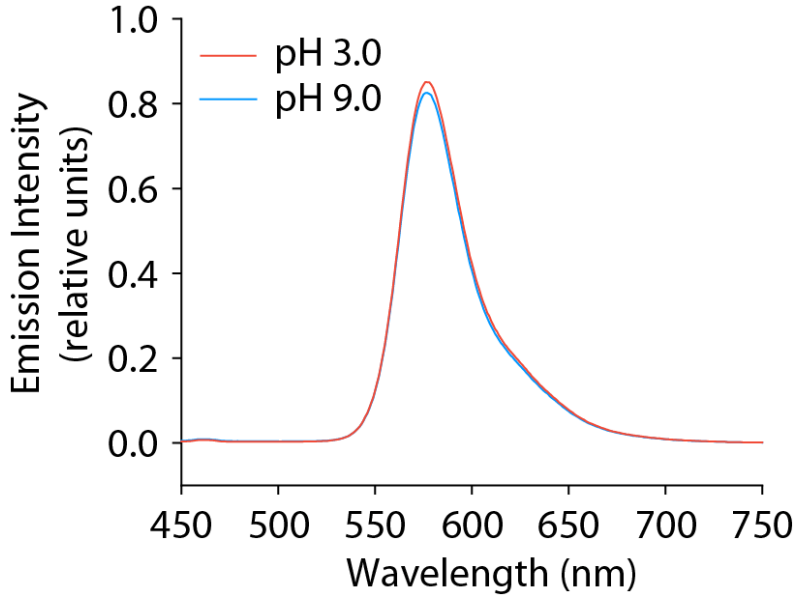

Fig. S21 pH-dependent emission spectra of RhB (10 μM).

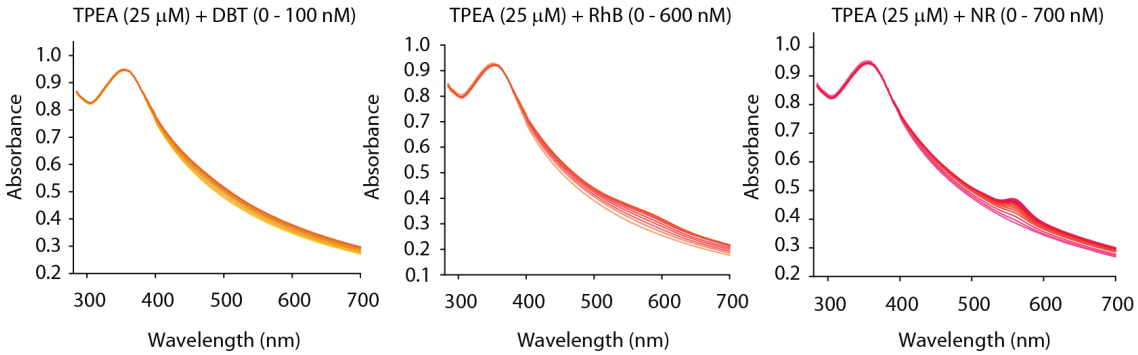

Fig. S22 Changes in the absorption spectra of TPEA (25 μM) upon addition of increasing concentrations of DBT, RhB and NR in pH 3.0.

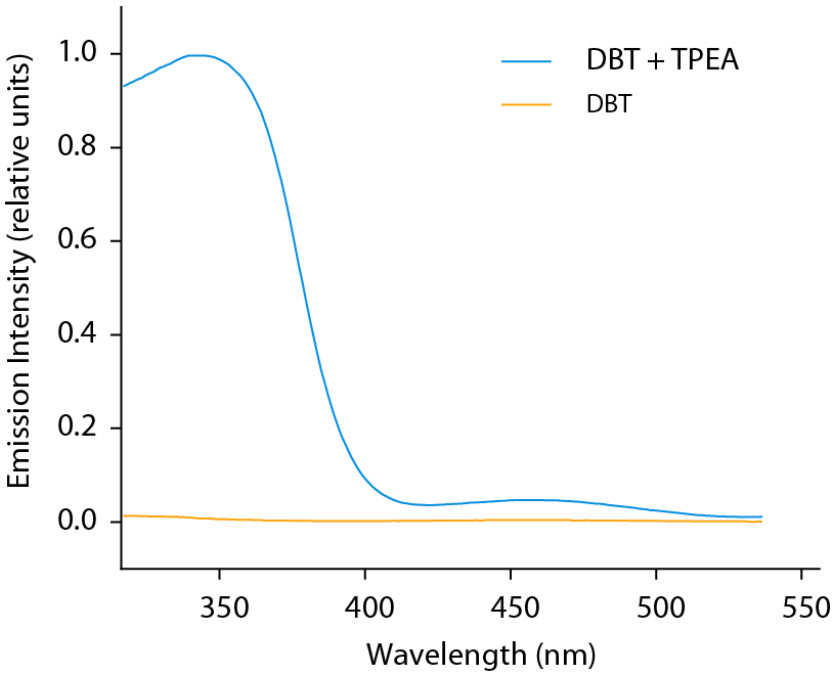

Fig. S23 Excitation spectra of DBT (100 nM, λ_{em} = 545 nm) in the absence and presence of TPEA.

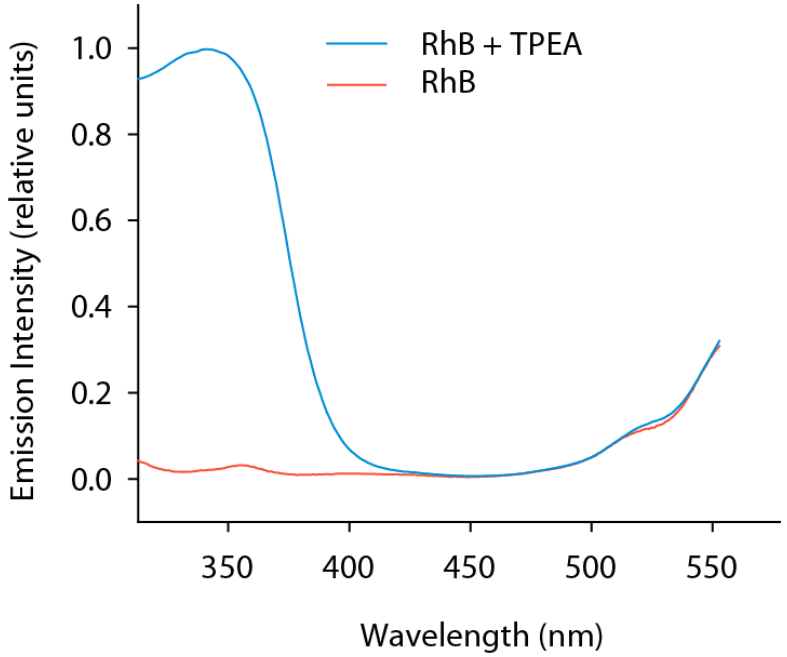

Fig. S24 Excitation spectra of RhB (600 nM, λ_{em} = 580 nm) in the absence and presence of TPEA.

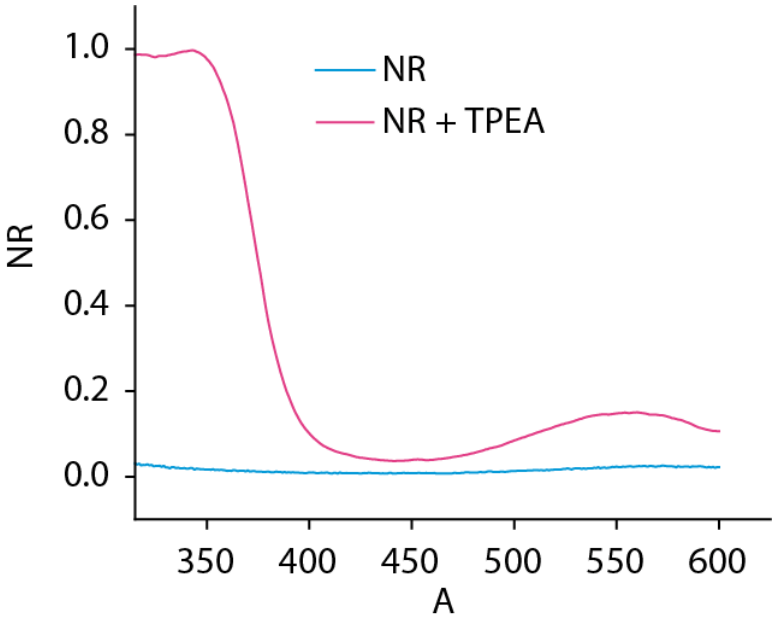

Fig. S25 Excitation spectra of NR (700 nM, λ_{em} = 615 nm) in the absence and presence of TPEA.

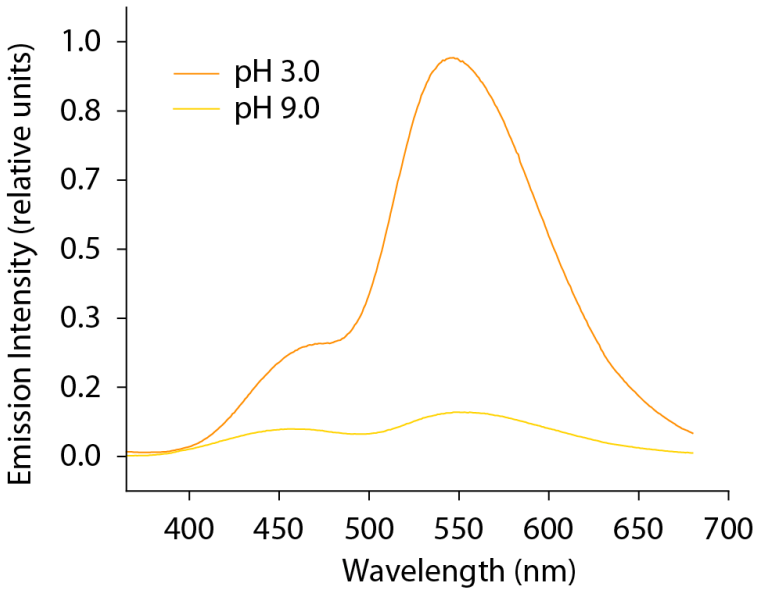

Fig. S26 pH-dependent emission spectra of TPEA with DBT

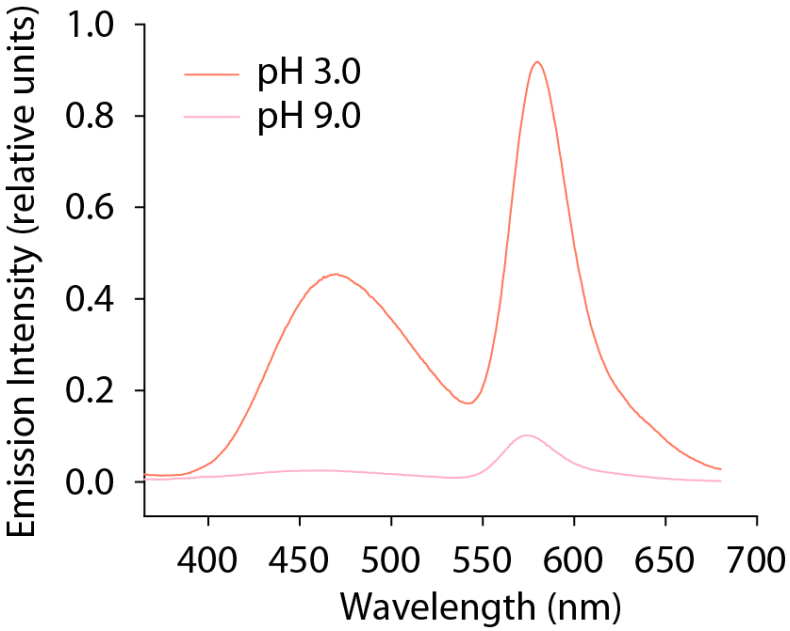

Fig. S27 pH-dependent emission spectra of TPEA with RhB

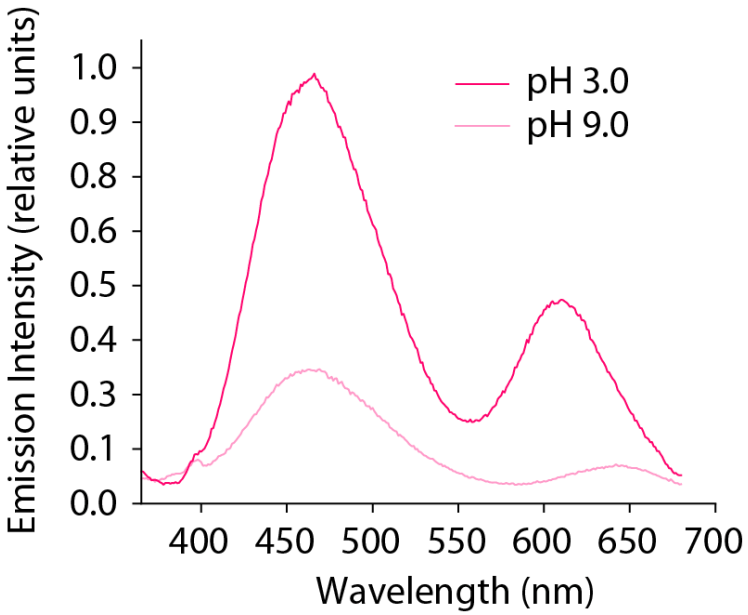

Fig. S28 pH-dependent emission spectra of TPEA with NR

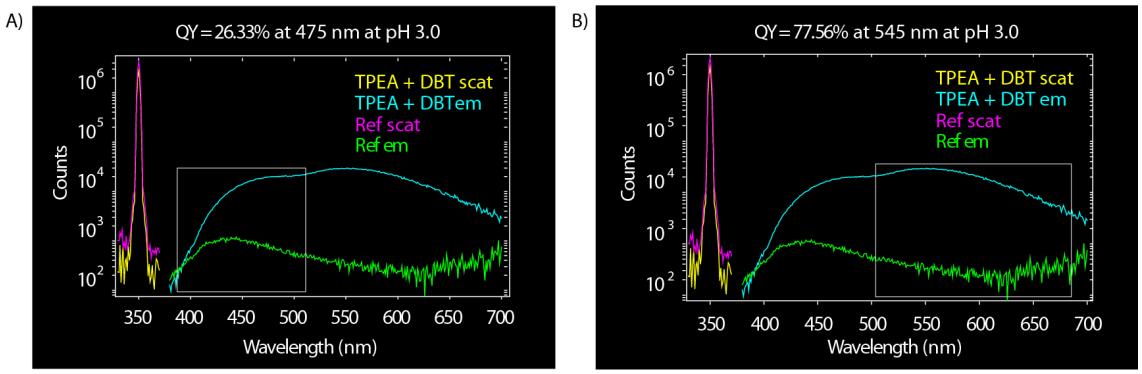

Fig. S29 Quantum yields at pH 3.0 for emission at A) 475nm for TPEA (25 μM) and at B) 545nm for DBT

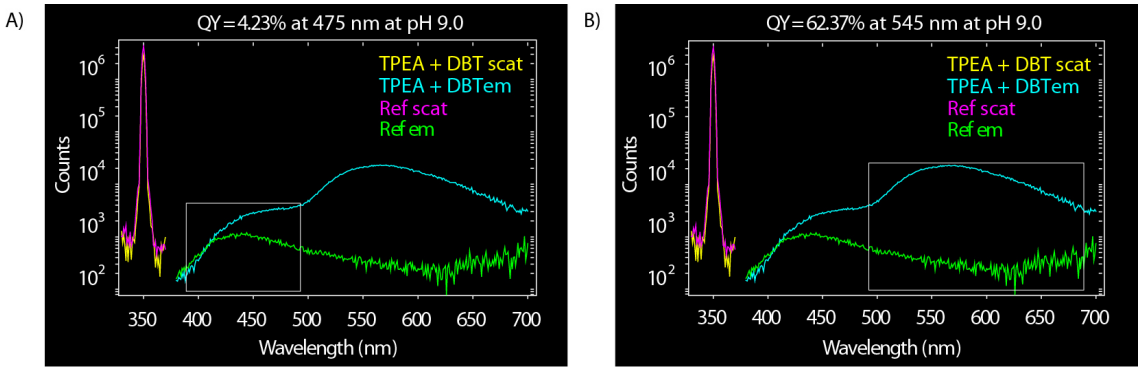

Fig. S30 Quantum yields at pH 9.0 for emission at A) 475nm for TPEA (25 μM) and at B) 545nm for DBT

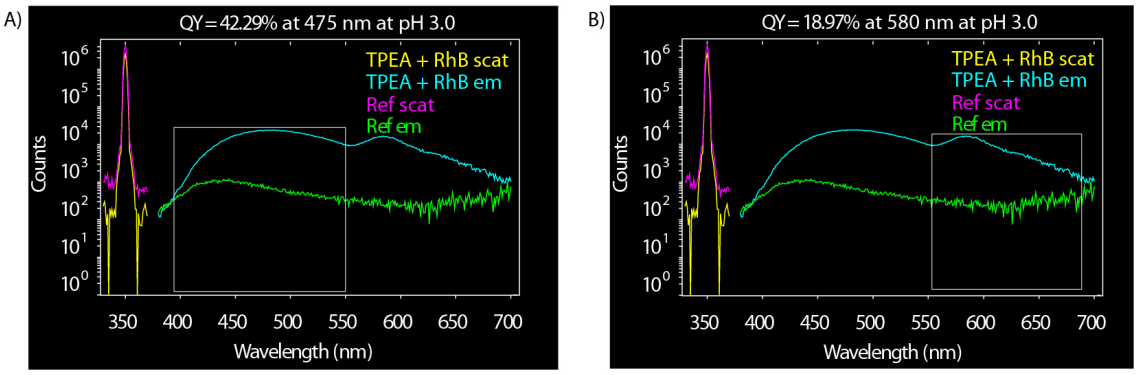

Fig. S31 Quantum yields at pH 3.0 for emission at A) 475nm for TPEA (25 μM) and at B) 580 nm for RhB.

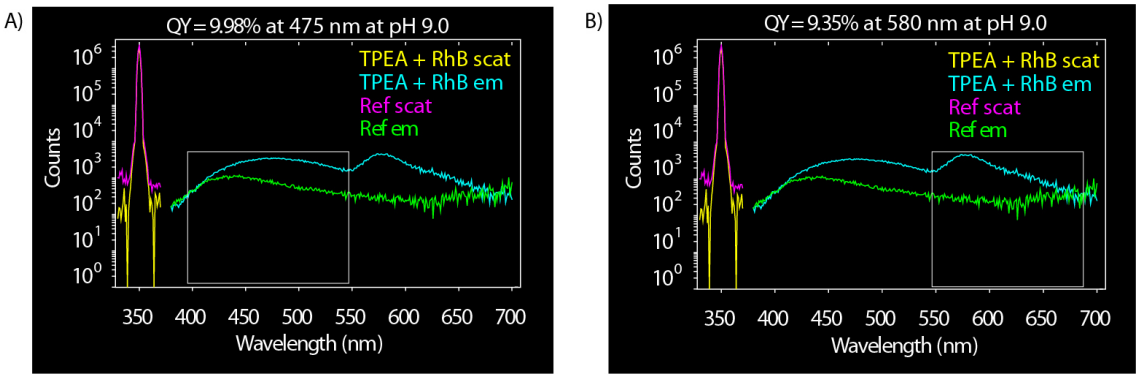

Fig. S32 Quantum yields at pH 9.0 for emission at A) 475nm for TPEA (25 μM) and at B) 580 nm for RhB.

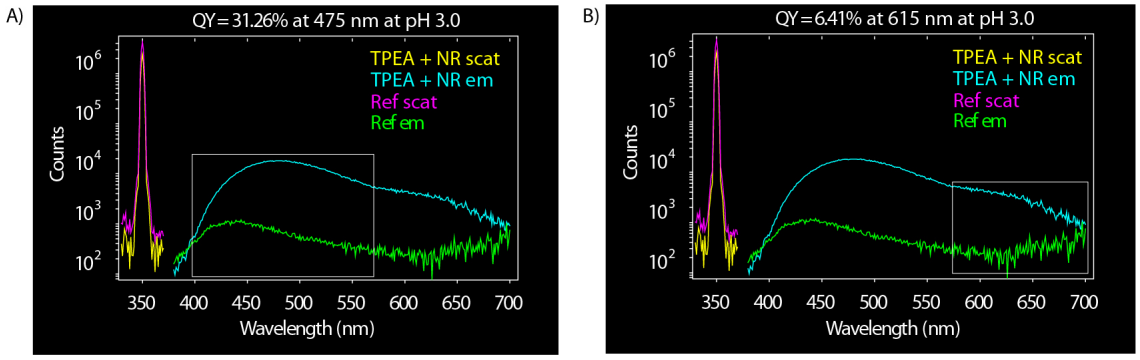

Fig. S33 Quantum yields at pH 3.0 for emission at A) 475nm for TPEA (25 μM) and at B) 615 nm for NR.

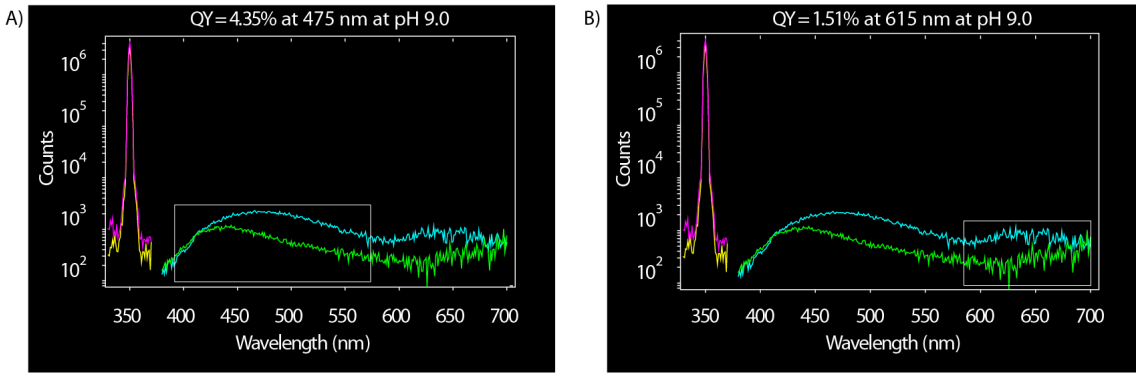

Fig. S34 Quantum yields at pH 9.0 for emission at A) 475nm for TPEA (25 μM) and at B) 615 nm for NR.

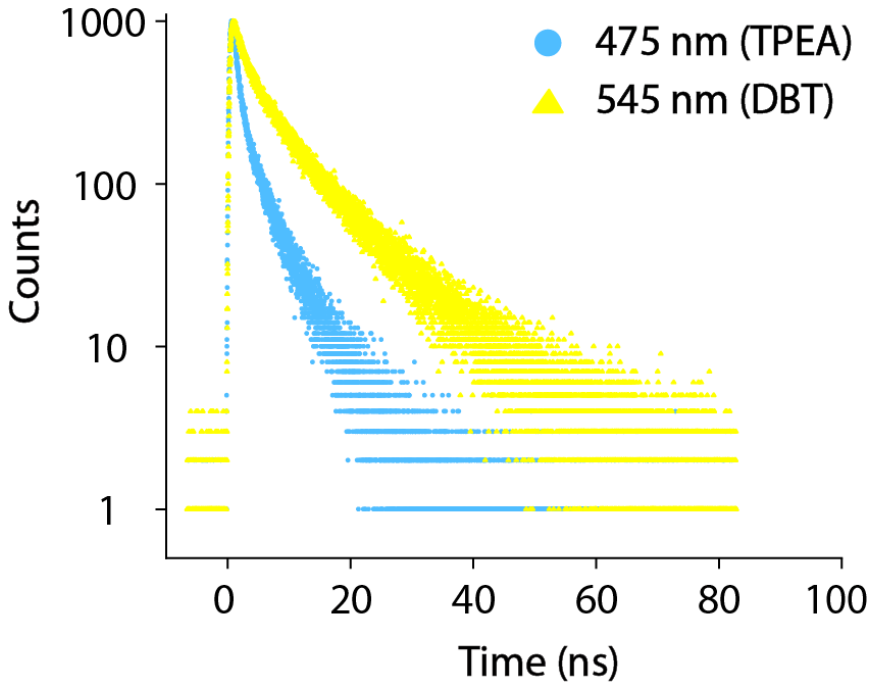

Fig. S35 Fluorescence decay profile of TPEA and DBT dye combination at pH 9.0.

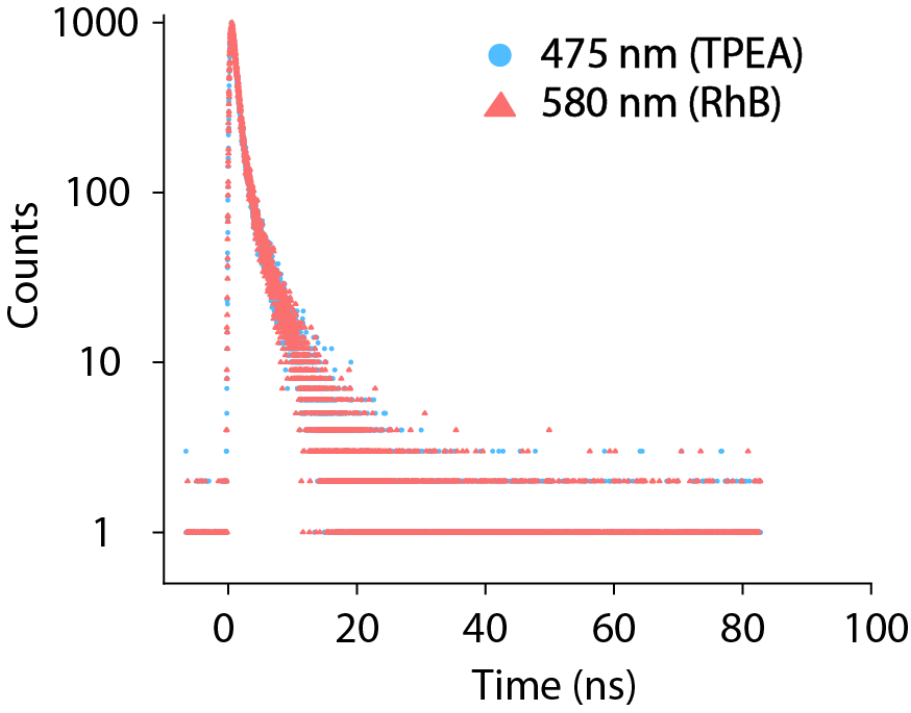

Fig. S36 Fluorescence decay profile of TPEA and RhB dye combination at pH 9.0.

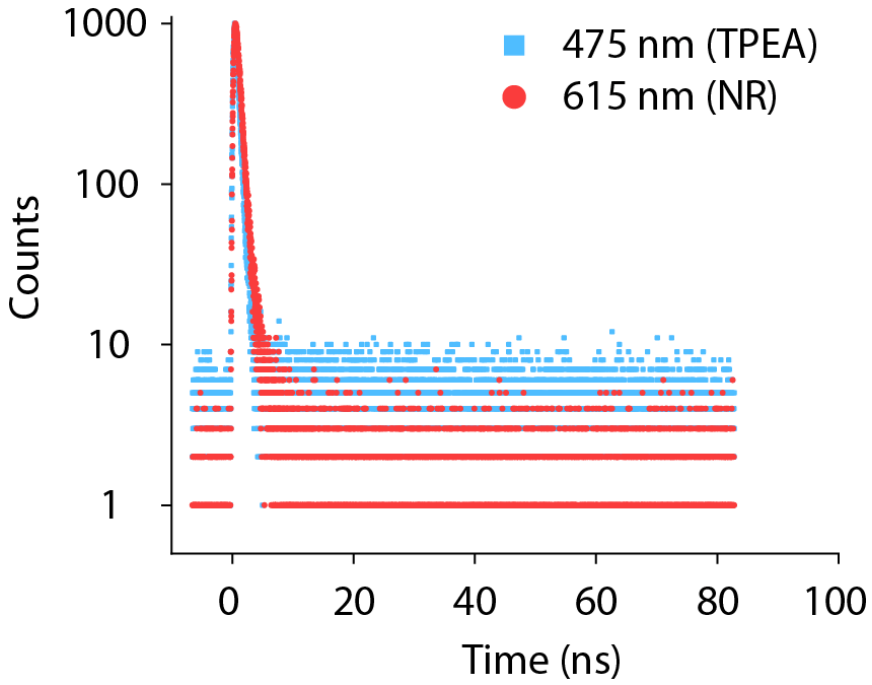

Fig. S37 Fluorescence decay profile of TPEA and NR dye combination at pH 9.0.

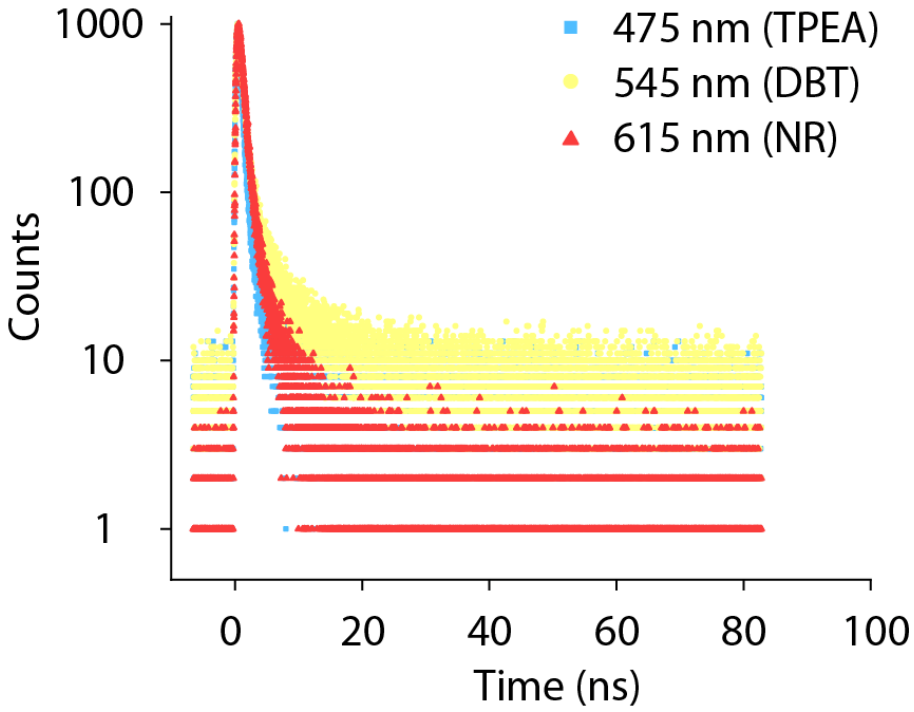

Fig. S38 Fluorescence decay profile of TPEA, DBT and NR dye combination at pH 9.0.

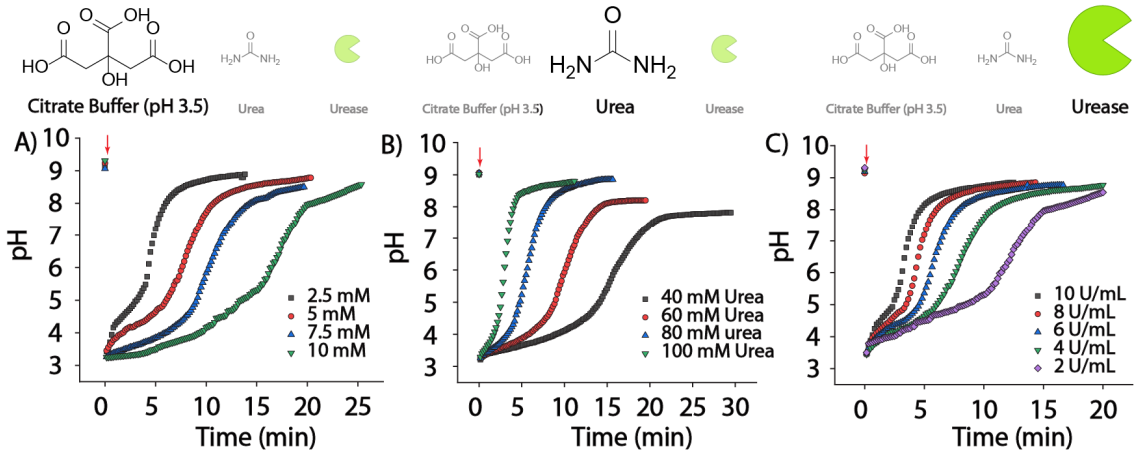

Fig. S36 Optimisation of citrate buffer-urea/urease pH clock. pH vs time profile with varying concentrations of A) citrate buffer under fixed concentrations of urea (100 mM) and urease (10 U/mL), B) urea under fixed concentrations of citrate buffer (10 mM) and urease (10 U/mL) and C) urease under fixed concentrations of citrate buffer (10 mM) and urea (100 mM). Additions of trigger have been indicated by the red arrows.

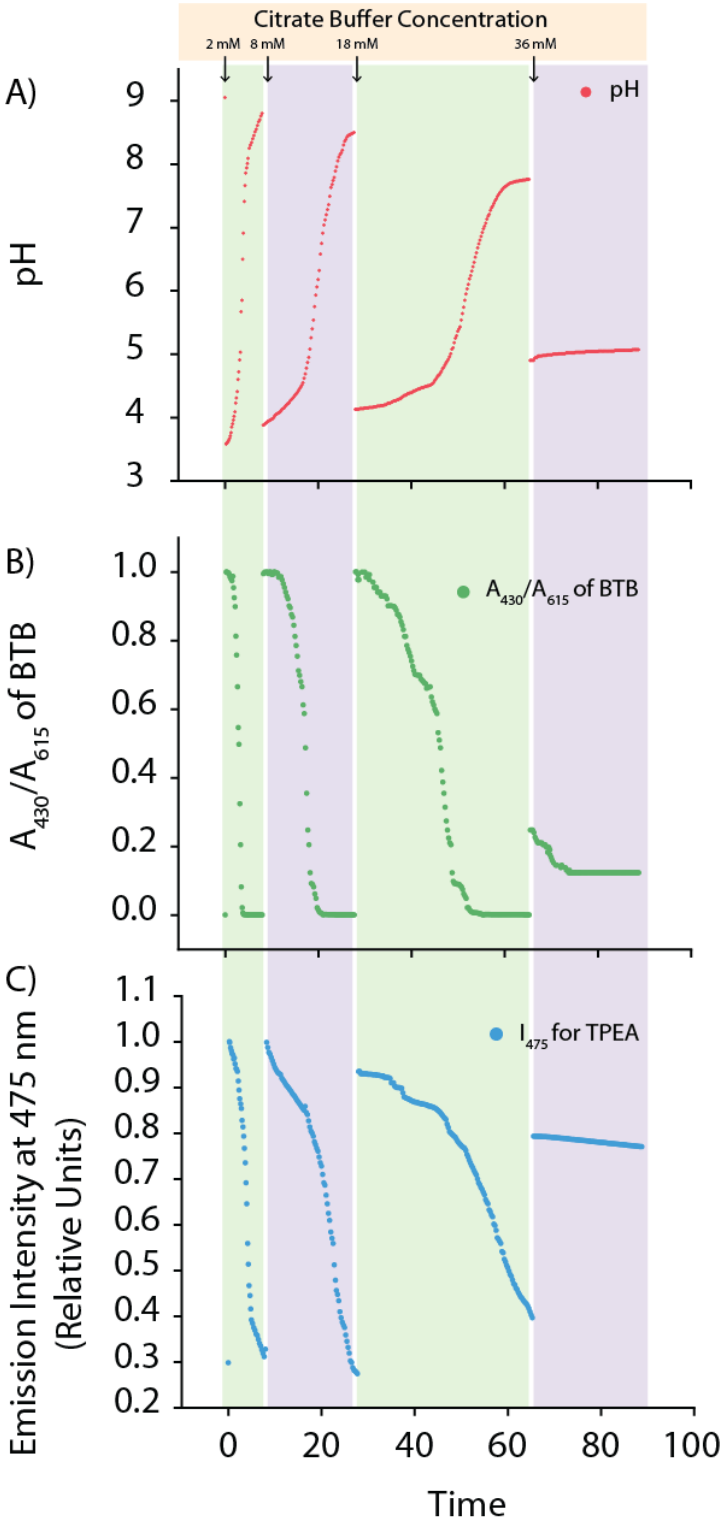

Fig. S37 Time-dependent A) pH profile, B) normalised absorbance ratio (A_{430}/A_{615}) of BTB (10 μM) and C) normalised emission intensity at 475 nm (I_{475}) of TPEA (25 μM) under mulitple cycles of pH clock repeated with subsequent additions of acid (citrate buffer, pH 3.5) trigger in a solution of urease (80 U/mL) with 120 mM urea. The time points and concentrations of the acid trigger added at every repetition are indicated by arrows at the top of the figure.

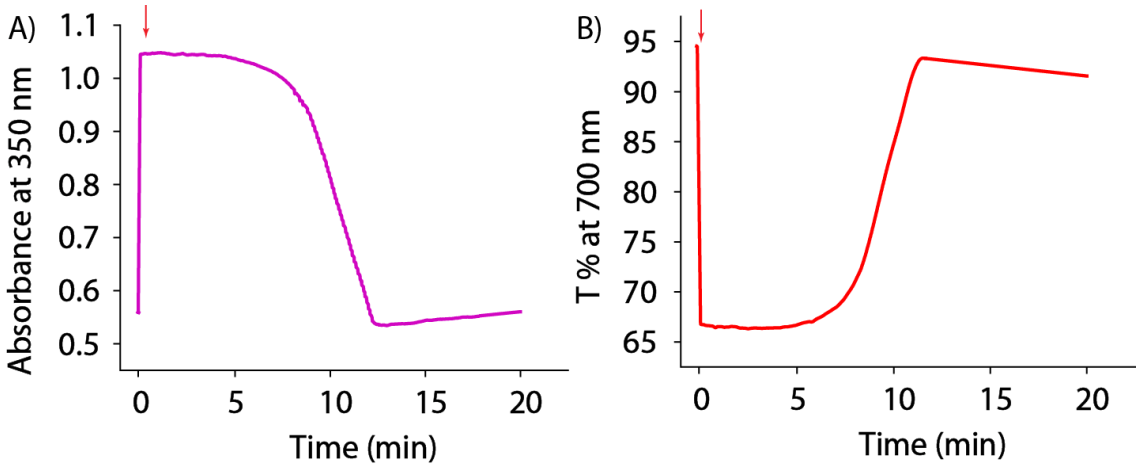

Fig. S38 Time-dependent A) absorption at 350 nm and B) transmittance (T%) at 700 nm for TPEA (25 μM) under pH clock. Additions of trigger have been indicated by the red arrows.

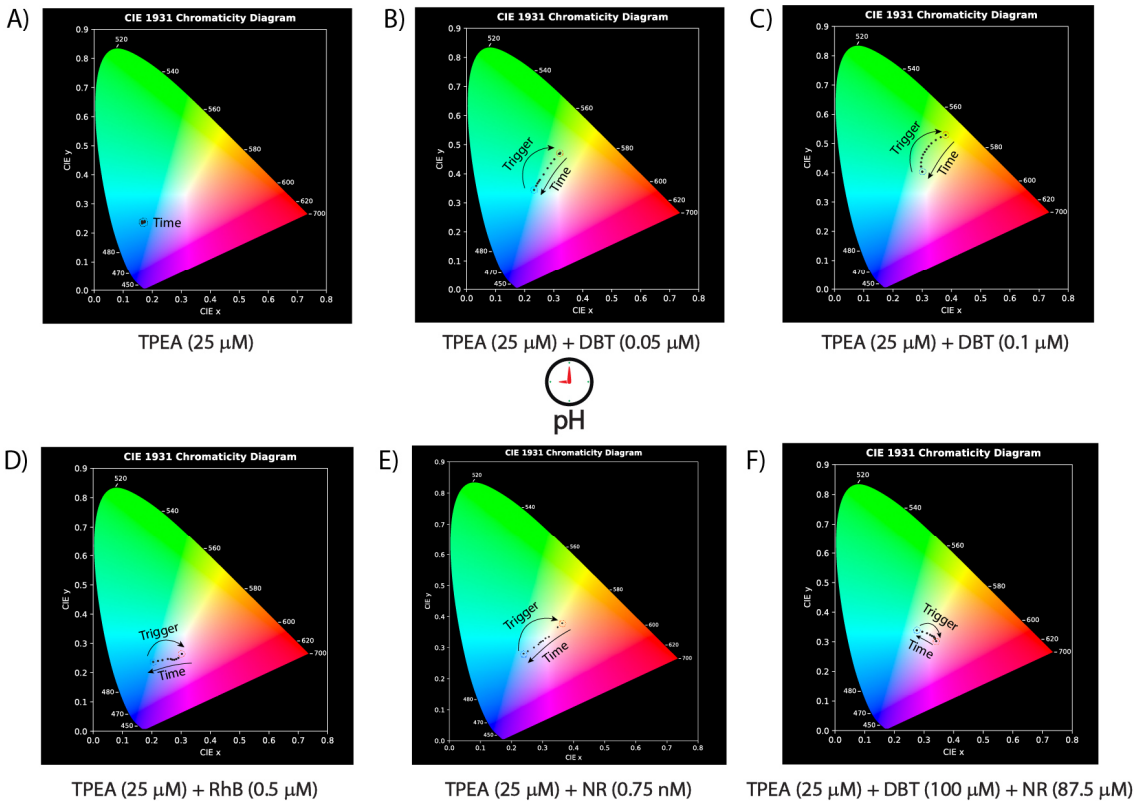

Fig. S39 Time-dependent CIE coordinates for the combination of dyes under the effect of the pH clock. The red and blue circled dots indicate the coordinates before and after the addition of the pH clock trigger.

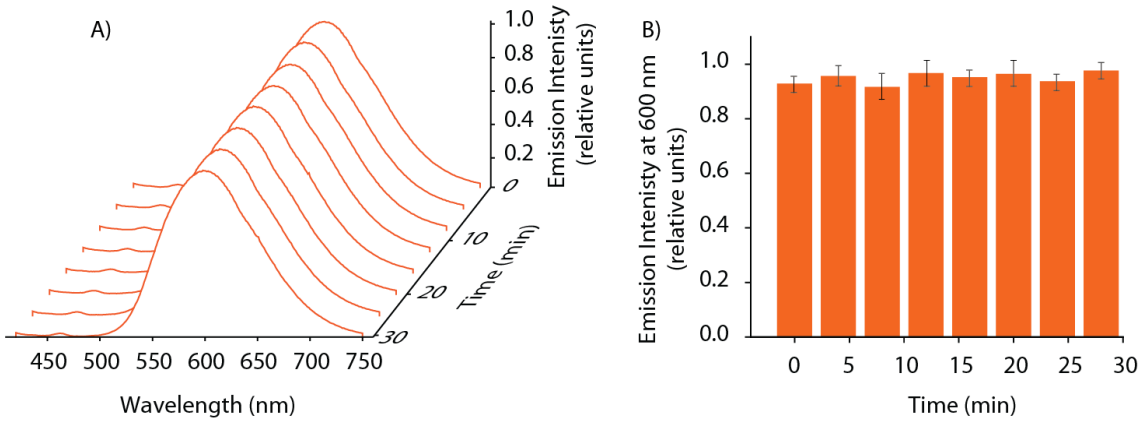

Fig. S40 A) Time-dependent emission spectra of DBT under the pH clock. B) Time-dependent emission intensity at 600 nm for DBT under the pH clock.

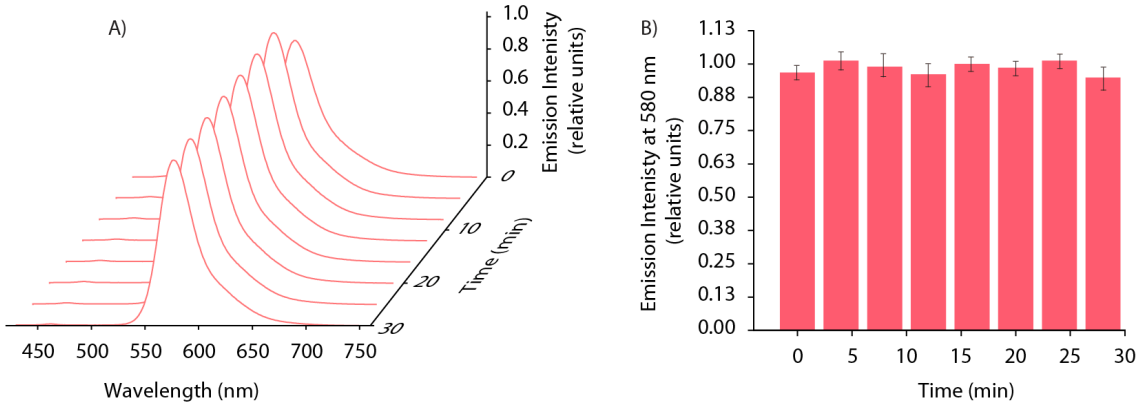

Fig. S41 A) Time-dependent emission spectra of RhB under the pH clock. B) Time-dependent emission intensity at 580 nm for RhB under the pH clock.

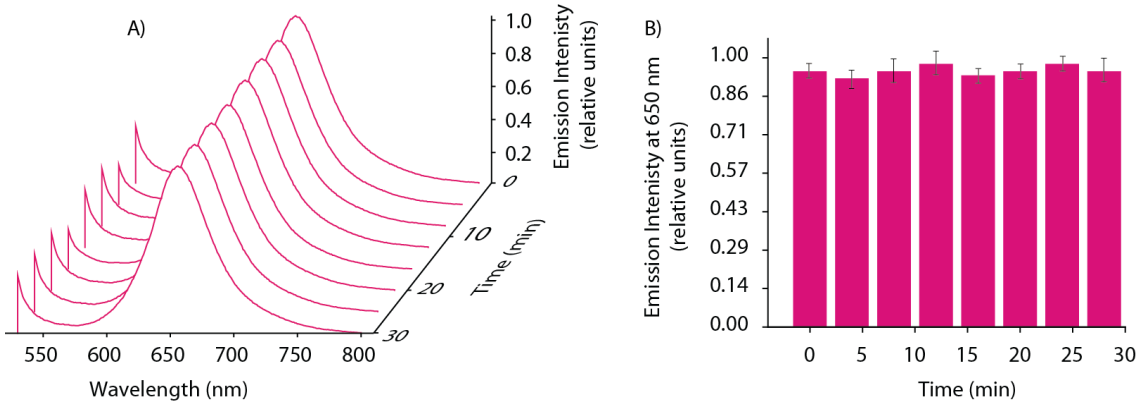

Fig. S42 A) Time-dependent emission spectra of NR under the pH clock. B) Time-dependent emission intensity at 650 nm for NR under the pH clock.

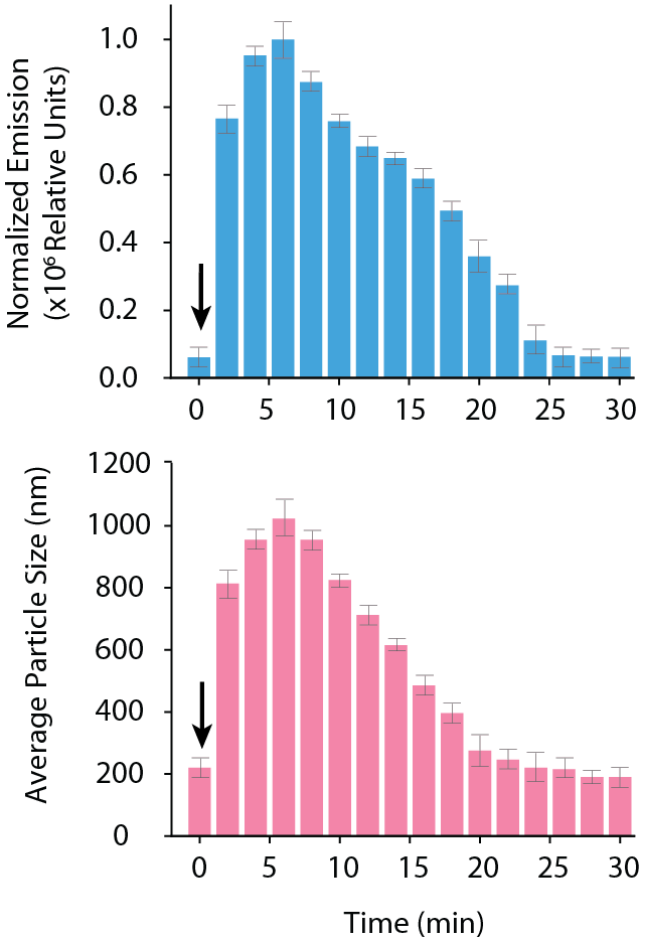

Fig. S43 A time-dependent correlation plot between emission of TPEA (25 μM) and particle sizes (nm) from DLS and under the effect of the pH clock. The arrow indicates the addition of the pH clock trigger

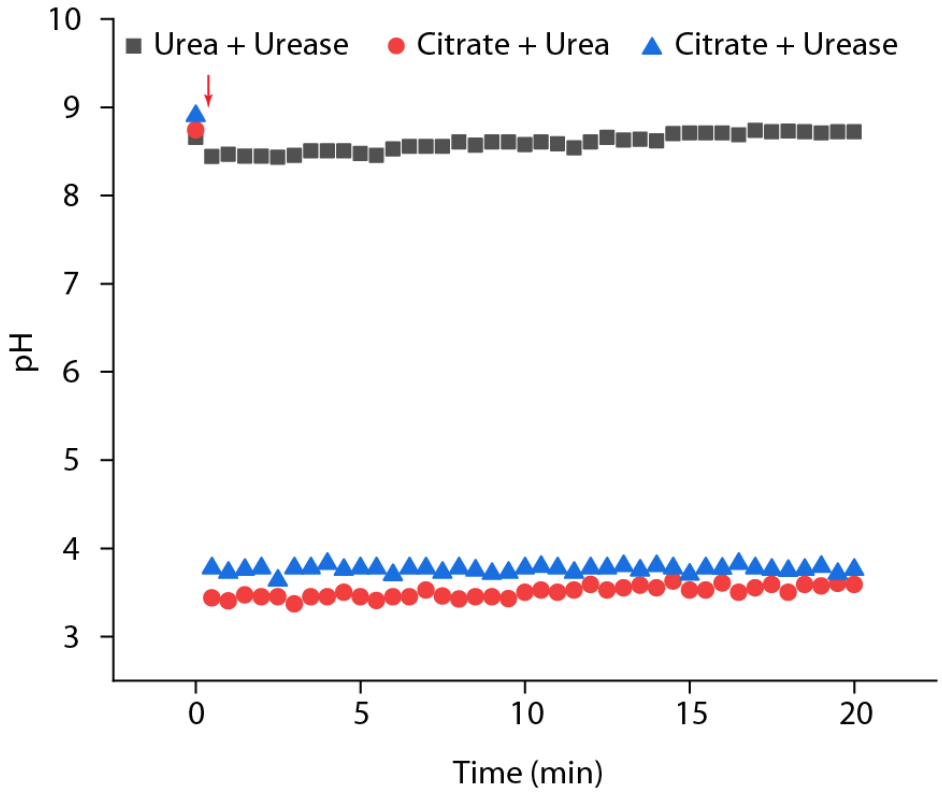

Fig. S44 pH clock control experiments. The addition of the pH-clock trigger is indicated by the red arrow.

Table S1. pH-dependent lifetime measurements of different combination of dyes

System	λ(nm)	pH	τ_1(ns)	τ_2(ns)	τ_{av}(ns)	χ^2
TPEA	475	3	0.89 (67%)	4.04 (33%)	1.92	0.99
		9	0.59 (86%)	5.41 (14%)	1.25	1.00
TPEA + DBT	475	3	3.18 (14%)	0.45 (86%)	0.84	1.22
		9	0.47 (88%)	4.58 (12%)	0.96	1.09
	545	3	2.33 (37%)	9.54 (63%)	6.87	1.11
		9	1.55 (66%)	9.97 (34%)	4.40	1.22
TPEA + RhB	475	3	2.18 (18%)	0.43(82%)	0.74	1.02
		9	0.33 (92%)	3.17 (08%)	0.54	0.98
	580	3	2.12 (87%)	3.90 (13%)	2.35	0.99
		9	0.35 (92%)	3.05 (8%)	0.58	0.96
TPEA + NR	475	3	0.63 (82%)	4.37 (18%)	1.30	0.99
		9	0.02 (49%)	0.02 (51%)	0.01	1.86
	615	3	0.94 (78%)	4.79 (22%)	1.77	1.04
		9	0.23 (92%)	0.99 (8%)	0.29	1.21
TPEA + DBT +NR	475	3	0.58 (83%)	4.36 (17%)	1.24	1.23
		9	0.12 (98%)	1.76 (2%)	0.15	1.37
	545	3	0.86 (76%)	4.99 (24%)	1.86	1.02
		9	0.28 (95%)	3.09 (5%)	0.41	1.38
	615	3	0.67 (84%)	4.44 (16%)	1.27	1.21
		9	0.33 (94%)	2.15 (6%)	0.45	1.26

Table S2. pH-dependent quantum yields of dye combinations.

System	λ(nm)	pH	Φ%
TPEA	475	3	67
		9	17
TPEA + DBT	475	3	26
		9	4
	545	3	77
		9	62
TPEA + RhB	475	3	42
		9	10
	580	3	19
		9	9
TPEA + NR	475	3	31
		9	4
	615	3	6
		9	1

Table S3. FRET efficiency for the combination of TPEA and DBT

TPEA (mM)	**DBT (nM)**	**I_{DA}**	**Φ_{ET} (%)**
25	0	1103780 (I_D)	-
25	12.5	886865.3	19.6
25	25	727730.9	34.0
25	37.5	636855.6	42.3
25	50	495792.3	55.1
25	62.5	402290.6	63.5
25	75	340864.7	69.1
25	87.5	273978.2	75.2
25	100	210732.1	80.9

Table S4. FRET efficiency for the combination of TPEA and RhB

TPEA (mM)	RhB (nM)	I_{DA}	Φ_{ET} (%)
25	0	1424870 (I_D)	-
25	50	1052460	26.1
25	100	903927.5	36.5
25	150	778403.4	45.4
25	200	678190.2	52.4
25	250	597430.1	58.1
25	300	516799.6	63.7
25	350	455255.5	68.0
25	400	406000.2	71.5
25	450	358336.2	74.9
25	500	319152.5	77.6

Table S. FRET efficiency for the combination of TPEA and NR

TPEA (mM)	NR (nM)	I_{DA}	Φ_{ET} (%)
25	0	1251290 (I_D)	-
25	100	996420.7	20.3
25	200	753464.9	39.7
25	300	572836.6	54.2
25	400	451794.1	63.9
25	500	358479	71.4
25	600	272357.4	78.2
25	700	205185.7	83.6
25	800	143539.2	88.5

Spectroscopic characterization of synthesized compounds

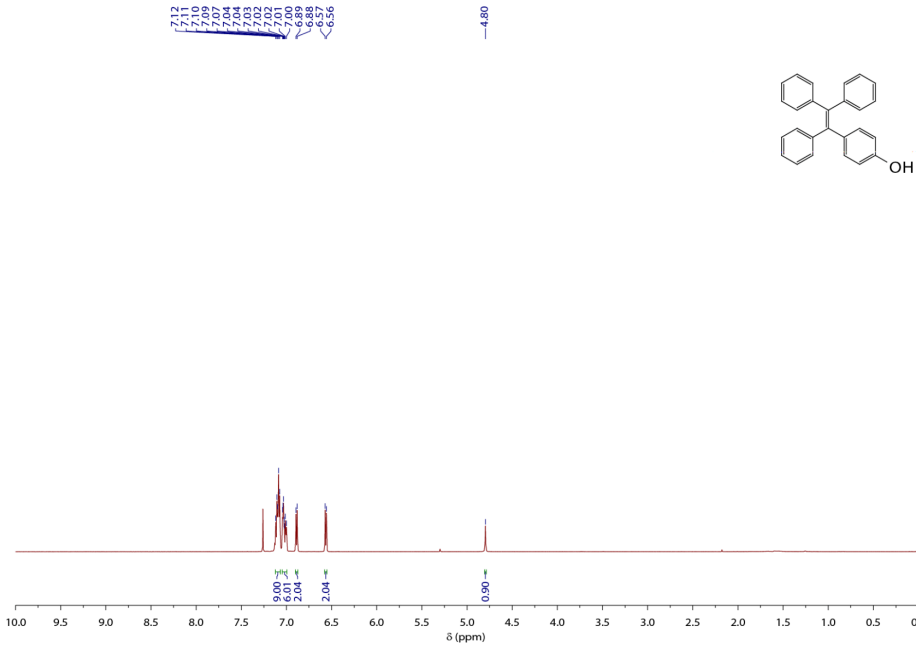

Fig. S39 ^{1}H NMR spectra of 1 in $CDCl_3$.

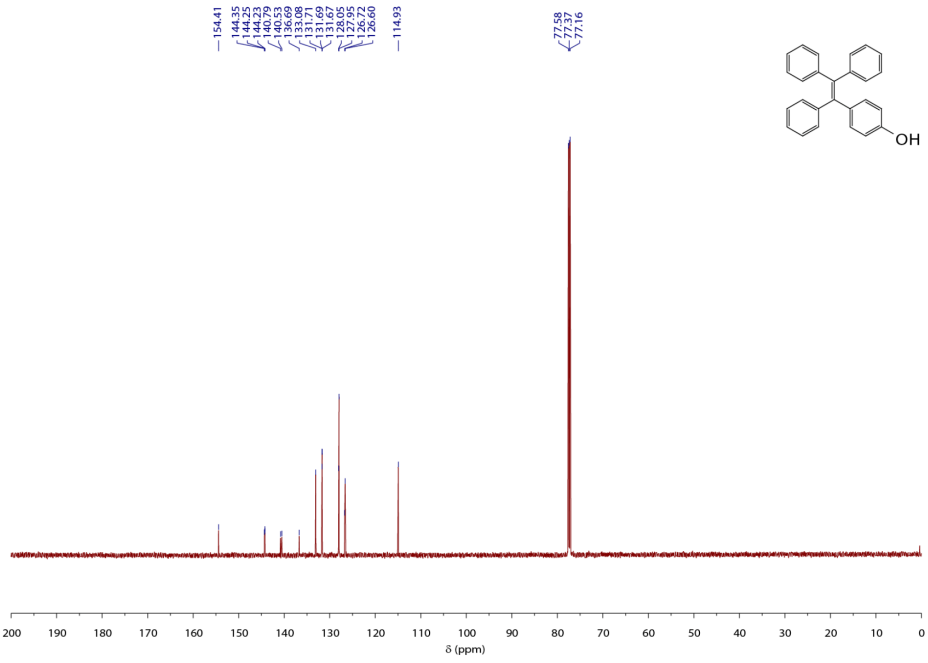

Fig. S40 ^{13}C NMR spectra of 1 in $CDCl_3$.

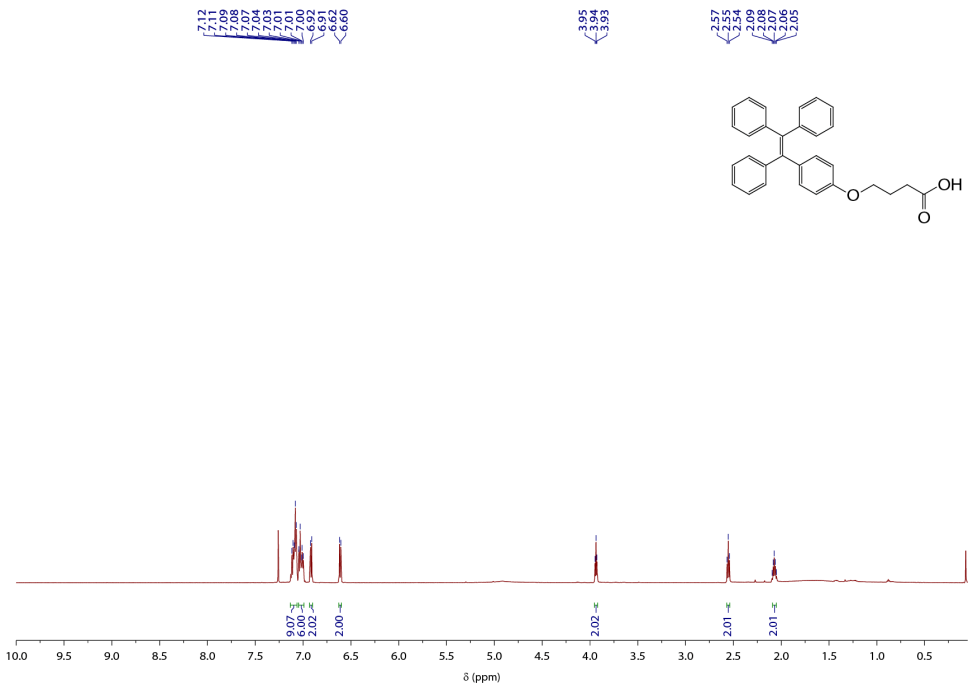

Fig. S41 ^{1}H NMR spectra of TPEA in $CDCl_3$.

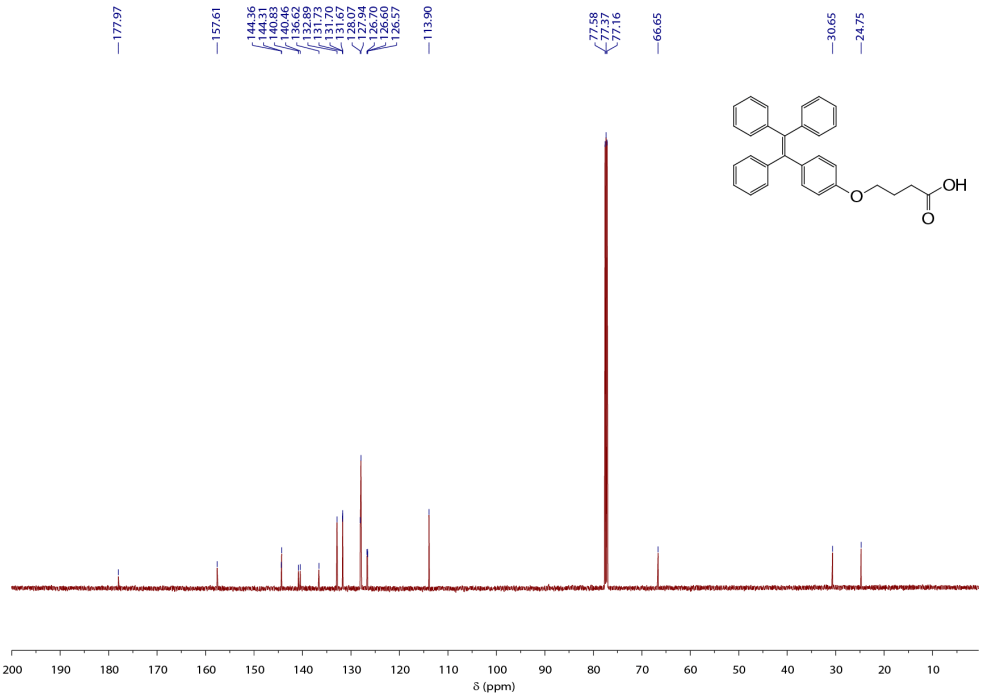

Fig. S41 ^{13}C NMR spectra of TPEA in $CDCl_3$.